

# Reversible lignin stabilization in traditional aqueous pulping conditions using boric acid

## Supporting Information

Zezhong John Li,<sup>a</sup> Ran Bi,<sup>b</sup> Songlan Sun,<sup>a</sup> Claire L.Bourmaud,<sup>a</sup> Shasha Zheng,<sup>a</sup> Matteo Darra,<sup>c</sup> Luana Amoroso,<sup>d</sup> Tiffany Abitbol,<sup>c</sup> Gustav Nyström,<sup>d</sup> Orlando J. Rojas,<sup>b</sup> Jeremy S. Luterbacher<sup>a\*</sup>

<sup>a</sup> *École Polytechnique Fédérale de Lausanne, Laboratory of Sustainable and Catalytic Processing, Station 6, Lausanne, 1015, Switzerland*

<sup>b</sup> *Bioproducts Institute, Department of Chemical and Biological Engineering, The University of British Columbia, Vancouver, BC V6T 1Z3, Canada*

<sup>c</sup> *Sustainable Materials Laboratory, Institute of Materials, School of Engineering, EPFL, Station 12, 1015 Lausanne, Switzerland*

<sup>d</sup> *Cellulose & Wood Materials Laboratory, Swiss Federal Laboratories for Materials Science and Technology (Empa), Überlandstrasse 129, 8600 Dübendorf, Switzerland.*

\* Corresponding author: [jeremy.luterbacher@epfl.ch](mailto:jeremy.luterbacher@epfl.ch) (Jeremy S. Luterbacher)

## Table of Contents

1.	Chemicals and materials.....	3
2.	Experimental methods.....	5
2.1	Lignin model compound reaction .....	5
2.2	Alkaline fractionation.....	5
2.3	Hydrogenolysis of extracted lignin .....	9
2.4	Reductive catalytic fractionation.....	9
2.5	Pulp and handsheet preparation.....	10
2.6	lignin solubility measurement .....	10
3.	Analytical methods.....	11
3.1	Compositional analysis of biomass and biomass liquors .....	11
3.2	Lignin monomer analysis by GC and GC-MS .....	14
3.3	NMR analysis of lignin or lignin model compounds .....	14
3.4	Pulp characterization .....	15
3.5	Handsheets characterization .....	15
4.	Supporting results and discussion .....	17
4.1	Lignin monomer identification and quantification.....	17
4.2	Fractionation and condition optimization in the 100 mL reactor .....	20
4.3	Lignin and xylan separation .....	29
4.4	Mass balance .....	31
4.5	Boric acid deprotection .....	34
4.6	Boric acid chemistry.....	36
4.7	Fractionation in the 1 L reactor .....	38
4.8	Pulp and handsheet characteristics .....	40
5.	Comparison with other fractionation technologies .....	44
6.	Lignin-based adhesive.....	45
7.	References .....	46

## 1. Chemicals and materials

All commercial chemicals were of analytical grade and were used without further purification.

- Hydrochloric acid (HCl), 37% wt/wt, Merck
- Sulfuric acid, 72 wt%, FisherScientific
- NaHCO<sub>3</sub>, >99%, Chemie Brunschwig
- MgSO<sub>4</sub> anhydrous, >99%, Reactolab S.A.
- 1,4-dioxane, ≥99.5%, stabilized by 250 ppm BHT, Carl Roth AG
- n-decane, analytical standard, Supelco
- Ru catalyst, 5% wt/wt Ru/C, Sigma-Aldrich
- NaOH, 1M solution, FisherScientific
- NaOH, pellets, Reactolab SA
- Boric acid, ≥99.5%, Carl Roth AG
- Methylboronic acid, 98%, Chemie Brunschwig
- n-Propylboronic acid, 98%, Chemie Brunschwig
- n-Butylboronic acid, 98%, Chemie Brunschwig
- Phenylboronic acid, 98% (may contain varying degrees of Triphenylboroxin), Chemie Brunschwig
- Dimethylsulfoxide-d<sub>6</sub> (DMSO-d<sub>6</sub>), Cambridge Isotope Laboratories.
- Chloroform-d, Cambridge Isotope Laboratories.
- Acetone, 99.9% HPLC grade, FisherScientific
- Isopropanol, 99.9% HPLC grade, FisherScientific
- Ethanol, 99.9% HPLC grade, FisherScientific
- Hydrogen peroxide, 30% in water, Reactolab S.A.
- 1,2,4,5-Tetrachloro-3-nitrobenzene (standard for quantitative <sup>1</sup>H NMR), Sigma-Aldrich
- 2,4,6-Triphenylboroxin, 96% (standard for quantitative <sup>11</sup>B NMR), Fluorochem
- Veratrylglycerol-β-guaiacyl ether, 97% (GC), Chemie Brunschwig
- MQ water was purified using a Millipore Milli-Q Advantage A10 water purification system to a resistivity higher than 18 MΩ.cm.
- North bleached Kraft pulp produced from birch and mixed softwood was provided by the UPM group in Finland.
- Kraft lignin (BioPiva 100) was provided by the UPM group in Finland.
- Xylose, 99%, Sigma-Aldrich
- Glucose, 99.5%, Sigma-Aldrich
- Arabinose, 98%, IVALUA
- Galactose, 99%, Sigma-Aldrich
- Mannose, 98%, Sigma-Aldrich

- Acetic acid, glacial, FisherScientific
- Furfural, 99%, Sigma-Aldrich
- 5-HMF, >99%, Sigma-Aldrich
- Calcium carbonate, >99%, Sigma-Aldrich

Biomass samples used in this study were provided by Dr. Michael Studer at Bern University of Applied Sciences (Switzerland). They were harvested in Switzerland, debarked, hammer milled into chips to pass through a 30 mm screen, and dried at 40°C. They were stored at ambient conditions in a sealed bucket after preparation.

- Beech (*Fagus sylvatica*): Harvested in Mühledorf, Bern, in winter, 2017/18.
- Birch (*Betula pendula*): Harvested in Solothurn, Solothurn, in June 2018.
- Spruce (*Picea abies*): Harvested in Messen, Solothurn, in winter 2019.
- Black pine (*Pinus nigra*): Harvested in Lausanne, Vaud, in summer 2018.

All wood chips were comminuted with a cutting mill to pass through a 6-mm screen for small batch reactions in the 100 mL reactor.

Alternatively, they were cut by hand to ca. 0.5 cm x 0.5 cm x 3 cm pieces for pulp production in the 1 L reactor.

The compositions of wood species are summarized in Table S1.

**Table S1.** Compositional analysis of biomass.

Species	Moisture (wt%) <sup>[a]</sup>	Weight fraction (wt%) <sup>[b]</sup>								
		Ext	Glu	Xyl	Gal	Man	Ara	KL	ASL	Acetyl
<b>Birch</b>	8.43	3.27	32.16	17.9	2.01	0.26	0.56	17.94	2.81	5.89
<b>Beech</b>	6.48	3.06	33.20	16.62	1.85	0.54	0.50	20.10	2.05	7.43
<b>Spruce</b>	0.37	4.95	40.65	6.28	1.18	12.12	1.40	23.29	ND	0.90
<b>Pine</b>	5.50	8.65	36.20	6.25	3.05	6.43	1.62	30.79	0.61	0.52

Notes: <sup>[a]</sup> On the basis of wet biomass, <sup>[b]</sup> on the basis of dried biomass

“Ext” refers to extractives; “Glu” refers to glucan; “Xyl” refers to xylan; “Gal” refers to galactan; “Man” refers to mannan; “Ara” refers to arabinan; “KL” refers to Klason lignin; “ASL” refers to acid-soluble lignin; and “ND” refers to not determined.

## 2. Experimental methods

### 2.1 Lignin model compound reaction

Veratrylglycerol- $\beta$ -guaiacyl ether (VG) (50 mg) was added in 1,4-dioxane (1.8 mL) with NaOH (40 mg) and phenylboronic acid (270 mg) in a 10 mL glass reactor. The mixture was heated in an oil bath at 80°C for 1 h. After the reaction was complete, the reaction mixture was neutralized with HCl (37%, 83.5  $\mu$ L) before the solvent was evaporated using a rotary evaporator at 45°C. A biphasic mixture of ethyl acetate (20 mL) and MQ water (10 mL) was added to redissolve the product. The organic layer was washed with 10 mL of MQ water once before drying with anhydrous MgSO<sub>4</sub>. The salt was removed with filtration, and the organic filtrate was dried with a rotary evaporator at 45°C. The residue was dissolved in deuterated chloroform for NMR analysis.

### 2.2 Alkaline fractionation

#### 2.2.1 100 mL reactor

##### 2.2.1.1 Single-pass fractionation

Wood chips (6 mm, 10 g) were loaded in a 100 mL pressure-tight steel reactor equipped with a pressure gauge and a K-type thermal couple with a NaOH aqueous solution (50 mL, 1 M) and boric or boronic acid (20 mmol, ca. 3.5 mol. eq. of the  $\beta$ -O-4 content in the wood chips). Soda control trials were conducted without boric or boronic acids. All fractionations were conducted without stirring to better capture behaviour in industrial digesters. The mixture was heated in the reactor to the desired internal temperature using a ceramic-lined heating mantle that was controlled with an FID temperature controller (Omega). It typically took 10 min to reach 130°C from room temperature and 17 min to reach 150-180°C. The reactor was held at that temperature for the specified residence time. Note that all residence times were assumed to start when the reactor internal temperature first reached the setpoint (the same protocol was used in all experiments in this work). When an impregnation step was used, the mixture was first left at 80°C for 2h before adjusting the heating controller to the fractionation temperature. Following the specified fractionation time, the reactor was cooled to room temperature by removing the heating mantel and blowing compressed air against the reactor. The cooling process typically took 15-20 min. The cellulose-rich solid and liquor fractions were separated by vacuum filtration using a 0.45  $\mu$ m PES membrane filter. The solid fraction was washed with MQ water until the pH was below 8. The liquor was acidified to pH 4 using HCl (37 wt.%). The precipitate of lignin and xylan was separated using a 0.45  $\mu$ m PES membrane filter. Without further drying or neutralizing HCl, the precipitate was dispersed in 1,4-dioxane (4mL) three times to dissolve lignin and remove insoluble xylan. The solid xylan and the lignin solution were eventually separated using a 0.8  $\mu$ m nylon membrane filter. The cellulose and xylan fractions were dried at 45°C and 50 mbar. If lignin were isolated as a solid instead of being analyzed by hydrogenolysis, acetone could also be used as the solvent to dissolve it from the co-precipitate. The filtrate was then dried to remove acetone. A small amount of NaHCO<sub>3</sub> (<0.01 g) was added to the mixture to neutralize acid and avoid acid-catalyzed lignin condensation when

lignin started to precipitate during evaporation while water (originally mixed with the co-precipitate) remained. Water was then fully evaporated. Lignin sample was further dried in vacuum oven at 50°C, 60 mbar overnight.

### 2.2.1.2 Cross-current configuration

Limited by the experimental setups in the lab, the three fractionation configurations were simulated by successively recycling the solid and liquor fractions and recombining them in designated sequences. In the cross-current case, to remove as much liquor as possible from the solid fraction, a centrifugal filter (PES, 0.45 µm) was used to separate the two phases after fractionation. The solid was fractionated with fresh liquor again without washing with water. The liquor phase was processed following the same procedure in 2.2.1.1. If not specified otherwise, the solid phase was fractionated in 4 sequential stages (Figure S1). This fractionation method was tested twice for reproducibility. This experiment used 6 mm birch chips in the 100 mL reactor. The chemical loadings in each stage were identical to the single-pass fractionation.

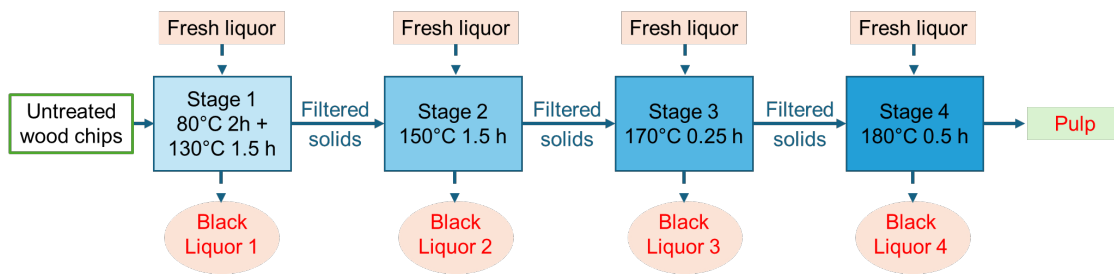


**Figure S1.** Process flow diagram of the cross-current configuration. The pulp and liquor fractions highlighted in red were collected for analysis.

### 2.2.1.3 Mixed-current configuration

As described in the main text, the mix-current configuration includes a step of cross-current digestion at 130°C (Stage 1 in Figure S2) and a counter-current section between 150°C and 180°C (Stages 2-4). At Stage 1, 50 mL fresh liquor with 1 M NaOH and 1.2 g of boric acid was used to fractionate raw wood chips after an impregnation step at 80°C for 2 h. The liquid and solid fractions were separated using a centrifugal filter (PES, 0.45 µm). This liquor fraction (Black Liquor 1 in Figure S2) was processed following the single-pass fractionation procedure. The solid fraction was passed down to the counter-current section.

A more elaborate fractionation sequence was developed to simulate the counter-current section. Another stream of 50mL fresh liquor with 1 M NaOH and 2 g of boric acid was added to digest the solid fraction at 150°C (Stage 2). Then the solid fraction was fractionated again with fresh liquor of the same composition at 170°C (Stage 3), and finally one more time at 180°C (Stage 4). The liquors from these steps were used to digest the wood fraction at a low temperature. For instance, liquor from the 170°C stage went to the 150°C stage, and liquor from the 180°C stage went to the 170°C stage. The solid going into the 150°C stage was always supplied from the cross-current 130°C stage, and it progressed sequentially to the stages at higher temperatures. This process continued until a liquor fraction was used to digest pulp at all three temperatures (i.e., 180°C – 170°C – 150°C, in sequence, e.g., Black Liquor 4 in Figure S2) and the wood was digested at all four temperatures (i.e., 130°C – 150°C – 170°C – 180°C, in sequence, Pulp 1 in

Figure S2). To assess reproducibility, the process was extended one round to obtain Black Liquor 5 and Pulp 2, shown in Figure S2. The mass balance was developed based on the untreated wood chips and fresh liquor streams as the incoming feed, and the Pulp 1 + Black Liquor 1 and 4, or Pulp 2 + Black Liquor 1 and 5, as the exiting streams (with each set being one of the duplicates). The other intermediate streams were not included in the mass balance, as these streams would occur within a reactor in a continuous setup. An average was taken from the two sets of duplicated outgoing streams. As this simulated process for a quasi-continuous setup was very time consuming, the experiment was stopped after Pulp 2 and Black Liquor 5 to obtain these duplicated results. Ideally, this process could be further repeated over many replicates to ensure a steady state or be tested in an actual continuous setup. Nevertheless, the delignification efficiency and lignin monomer yields were very similar between the duplicates in this work (Table S4, entries 25-26 vs 27-28, a difference of about 1% of the total monomer yields and in delignification efficiency), showing that with the limited replicates, we closely approximated the steady state regime. Mass balance in this work considered Klason lignin, glucan, xylan, galactan, arabinan, mannan, and acetyl from biomass as well as boric acid added in the fresh liquor, with the results summarized in Tables S8 and S10. This experiment used 6 mm birch chips in the 100 mL reactor.

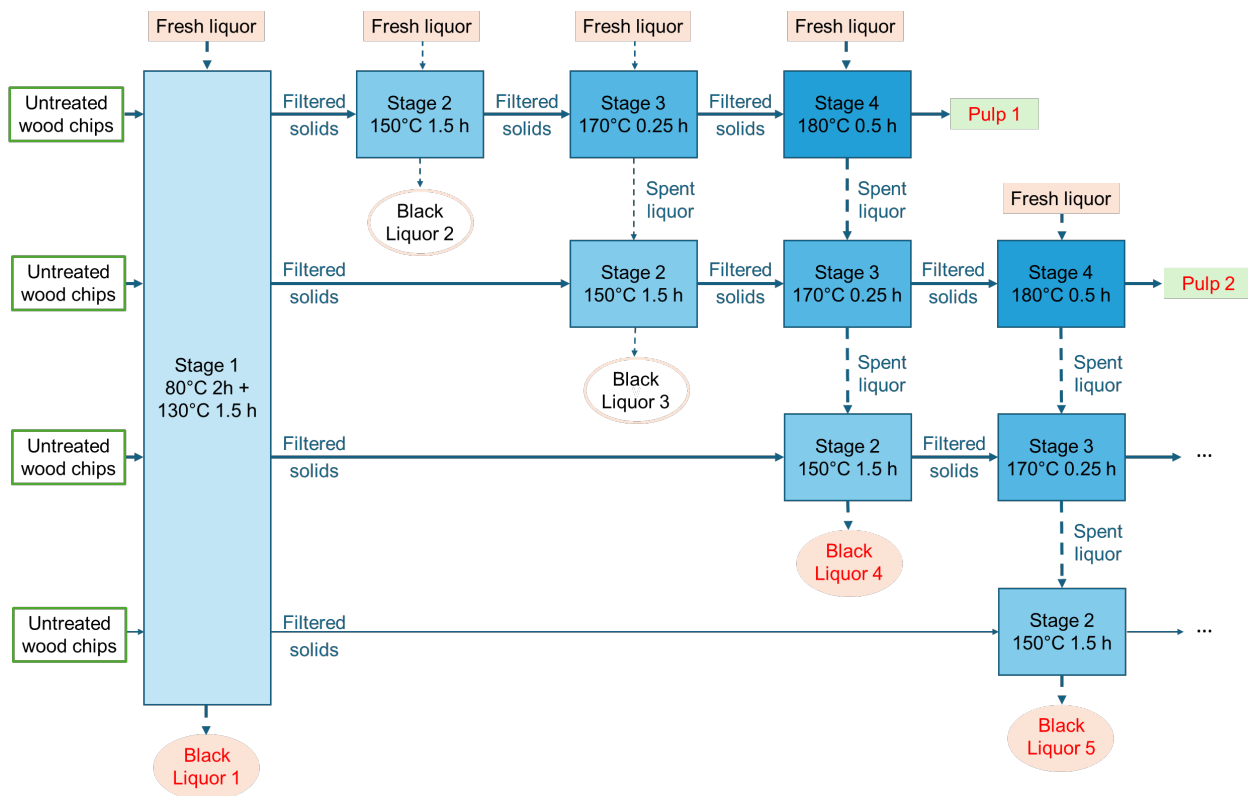


**Figure S2.** Process flow diagram of the mixed-current configuration. The pulp and liquor fractions highlighted in red were collected for analysis.

#### 2.2.1.4 Counter-current configuration

The counter-current configuration was conducted in the same manner as in the counter-current section (150-180°C) of the mixed-current configuration, except extending the use of recycled liquor to the impregnation at 80°C and the

130°C fractionation stage (Stage 1, Figure S3). Liquor from the 150°C stage was used to digest raw wood chips in Stage 1. This process continued until a liquor fraction was used to digest pulp at all four temperatures (i.e., 180°C – 170°C – 150°C – 130°C, in sequence, e.g., Black Liquor 4 in Figure S3) and the wood was digested at all four temperatures (i.e., 130°C – 150°C – 170°C – 180°C, in sequence, Pulp 1 in Figure S3). To assess reproducibility, the process was extended one round to obtain Black Liquor 5 and Pulp 2, shown in Figure S3. Similar to the mixed current configuration, the mass balance was developed based on untreated wood chips and fresh liquor streams as the incoming feed, and the Pulp 1 + Black Liquor 4, or Pulp 2 + Black Liquor 5, as the existing streams (duplicates). The delignification efficiency and lignin monomer yields were similar (a difference of about 3% of the total monomer yields and <1% delignification efficiency) between the duplicates in this work (Table S4, entry 33 vs 34), again showing that with the limited replicates, we closely approximated the steady state regime. The mass balance results are summarized in Tables S9 and S11. This experiment used 6 mm birch chips in the 100 mL reactor.

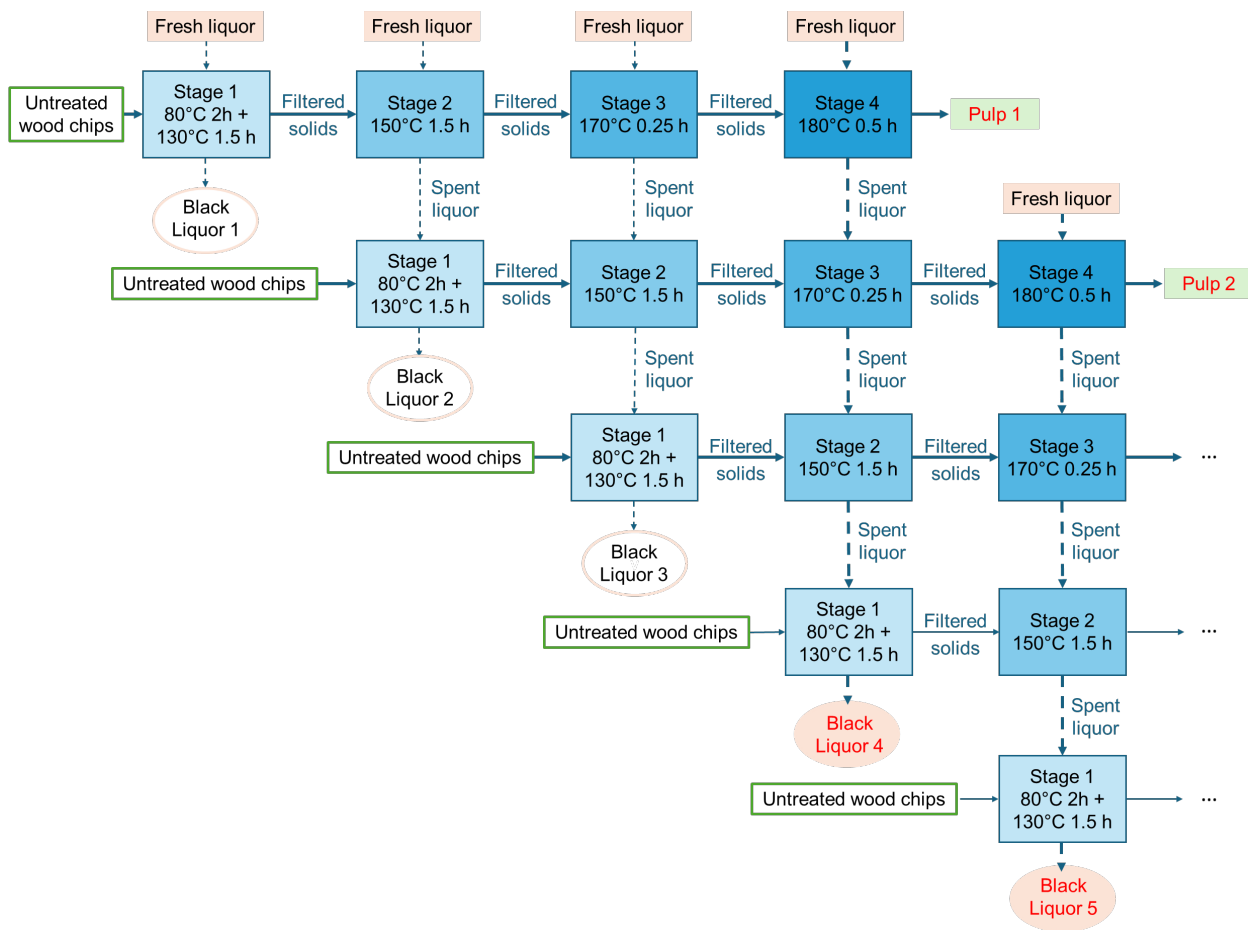


**Figure S3.** Process flow diagram of the counter-current configuration. The pulp and liquor fractions highlighted in red were collected for analysis.

### 2.2.2 1 L reactor

Pulp production in the 1 L reactor only followed the cross-current method for simplicity. For this large-scale run, wood chips were cut by hand into thick matchsticks (ca. 0.5 cm x 0.5 cm x 3 cm) to make sure the initial chip size would

not affect the pulp fibre dimensions. Birch chips (120 g), boric acid (14.64 g), and 700 mL of NaOH solution (1 M) were loaded in the 1 L pressure-tight Parr reactor equipped with a K-type thermal couple, a pressure gauge, and an overhead mechanical stirrer. The reactor was heated with a heating mantle, and the internal temperature was controlled by a PID controller (Omega). The fractionation sequence and workup procedure followed the small-scale cross-current method shown in Figure S2. One deviation was that a cellulose filter was used instead of membrane filters to improve efficiency. A gentle stirring at ca. 60 rpm was also used to improve heat transfer inside this 10-times larger reactor. The pulp fibres were washed with reverse osmosis (RO) water until pH<8, which was then drained through the filtration system using vacuum. A small sample (ca. 5 g oven-dry mass) was taken from the filter cake before the remainder was bleached. (*vide infra*).

In the case of spruce fractionation, 76 g of spruce matchsticks and 10 g of boric acid were added to 700 mL of NaOH solution (1M). The rest of the procedure remained unchanged. A smaller amount of spruce was used due to limited availability. Boric acid was scaled accordingly. The total liquor volume was kept unchanged due to the minimum volume of reaction mixture needed to keep the thermal couple submerged under the liquid surface. A detailed comparison with fractionation in a 100 mL reactor is given in Section 4.7, where lignin monomer yields, delignification efficiency, pulp compositions and properties are discussed. But overall, delignification efficiency and cellulose compositions were very similar across both scales.

### 2.3 Hydrogenolysis of extracted lignin

The lignin solution was diluted to 25 mL with 1,4-dioxane. A sample (3.5 mL) was added to a 50-mL Parr reactor along with 100 mg of catalyst (5 wt% Ru/C), 1,4-dioxane (16.5 mL), and HCl (20  $\mu$ L). The reactor was pressurized with 40 bar of H<sub>2</sub>. The reactor was heated to an internal temperature of 250°C and held at this temperature for 3 h with stirring at 400 rpm. After reaction, the reactor was cooled to room temperature and a known quantity of n-decane internal standard (0.2 mL, 0.04 g/mL) was added. A sample of the resulting liquid was neutralized with NaHCO<sub>3</sub> and then dried with anhydrous MgSO<sub>4</sub>. The said sample was taken for GC analysis after removing solid particles with a 0.2  $\mu$ m PTFE filter. The monomer yield was calculated based on the effective carbon numbers (detailed in section 4.1).

### 2.4 Reductive catalytic fractionation

RCF was performed in a stirred 50 mL-PARR reactor. Ball-milled biomass (1.5g) was added with 100 mg of catalyst (5 wt% Ru/C) and 1,4-dioxane (20 mL). The system was pressurized with 40 bar H<sub>2</sub>. The reactor was then heated to an internal temperature of 250°C and held at this temperature for 15 h with stirring. After reaction, the reactor was cooled to room temperature and an n-decane internal standard (0.2 mL, 0.04 g/mL) was added. A sample of the resulting liquid was taken for GC analysis after removing solid particles with a 0.2  $\mu$ m PTFE filter. The monomer yield was calculated based on the effective carbon numbers (detailed in section 4.1).

## 2.5 Pulp and handsheet preparation

### 2.5.1 Pulp bleaching

The pulp cake was mixed with the bleaching agent (5%  $\text{H}_2\text{O}_2$  in NaOH aqueous solution, pH=12) to achieve a final consistency of 10%. The mixture was placed in zipper-sealed polypropylene (PP) bags and heated in a thermostatic water bath at 70°C for 1 h. The bleaching solution was removed with vacuum filtration using a cellulose filter on a Buchner funnel. This process was repeated once. The bleached pulp cake was finally diluted with 0.1M NaOH solution to 10% consistency and heated at 70°C for 1h inside a zip-sealed PP bag in a water bath. The base wash was removed by filtration, and the bleached pulp was washed with RO water until a pH<7.2 was reached with the filtrate. The pulp cake was oven-dried at 105°C to measure the pulp yield.

### 2.5.2 Handsheet manufacture

All dried pulp samples were hand torn into small pieces and rehydrated by soaking in MQ water for 5 h. The mixture was disintegrated at a 1% consistency for 60,000 revolutions using a pulp disintegrator (Frank-PTI). The suspension was diluted to 0.3% with RO water for storage.

The pulp handsheets were made using an automated sheet former of a 20 cm nominal diameter (Rapid- Köthen, Frank-PTI). The pulp suspension was evenly sampled and massed with a targeted dry mass of 1.9 g. The mass was selected to achieve a grammage of 60g/m<sup>2</sup>, which corresponds to the ISO and TAPPI standard for handsheet mechanical tests.<sup>1,2</sup> The pulp suspension was added to tap water to reach a total volume of 7 L. The water was drained through a fine screen, above which fibres were retained. The pulp pad on the screen was transferred between two pieces of blotting paper and dried at 98°C, 0.1 bar for 9 min. The dry mass of each handsheet was measured, and the corresponding grammage was calculated.

## 2.6 lignin solubility measurement

The isolated lignin (ca. 0.2 g), either BAF lignin, soda control lignin, or Kraft lignin, was mixed with 0.5 mL of 1M NaOH solution. As the boric protection was removed by acidification, 0.012 g of boric acid was added to the BAF lignin mixture to achieve the same environment as in the BAF liquor during fractionation. All mixtures were sonicated at room temperature and centrifuged to precipitate the undissolved lignin fraction. 0.1 mL of the supernatant was reprecipitated in pH 3 water acidified with HCl over a dried and tared centrifugal filter. The mass of transferred supernatant was also recorded. The lignin precipitate was separated from water in a centrifuge and dried in a vacuum oven overnight. All experiments were conducted in duplicates to estimate the error margin.

### 3. Analytical methods

#### 3.1 Compositional analysis of biomass and biomass liquors

The compositions of raw wood chips, fractionated cellulose residues, and the clean liquor after separating lignin and xylan were quantified following the standard procedure published in *Nature Protocols*<sup>3</sup>, which is based on the procedure from the US National Renewable Energy Laboratory (NREL).<sup>4</sup> Briefly, ca. 1.2 g of solid samples were pulverized in a ball mill (Restch) with a 50 mL ZrO<sub>2</sub>-lined grinding jar and 20 ZrO<sub>2</sub> grinding balls of 1 cm in diameter (ca. 63 g in total). Milling was performed at 450 rpm for 1 h with 5 min on-off cycles. The powder was stored at 45°C and 45 mbar overnight to remove moisture. Approximately 0.3 g of the dehydrated sample was dispersed in 4.5 mL of 72 wt% H<sub>2</sub>SO<sub>4</sub> and digested below 35°C for 1 h in a sonicating water bath. The mixture was then diluted with MQ water to 180 mL to a final acid concentration of 4 wt% and digested again at 120°C for 1 h. The insoluble precipitate was filtered out and designated as Klason lignin. The hydrolysate was diluted to 250 mL with MQ water, and its compositions were quantified using high-performance liquid chromatography (HPLC) (Agilent Infinity 1260). Specifically, acetic acid and boric acid were quantified using an Aminex HPX-87H Column (300 mm x 7.8 mm, column temperature = 60 °C) using pH 2 water as eluent (flow rate = 0.6 mL·min<sup>-1</sup>, Vinj = 20 µL) with a Refractive Index Detector (RID). Furfural and 5-HMF were quantified using the same column but with a diode-array detector (DAD) at 260 nm wavelength. An aliquot of the hydrolysate was then neutralized with CaCO<sub>3</sub> and taken for sugar quantification after removing the solid. Sugar compositions were measured using the same HPLC stack but with an Aminex HPX-87P Column (300 mm x 7.8 mm, column temperature = 80 °C) using MQ water as eluent (flow rate = 0.6 mL·min<sup>-1</sup>, Vinj = 20 µL) with a RID. To calculate yields, measured quantities of sugar monomers were converted to those of the respective polysaccharides, accounting for the mass difference due to dehydration during polysaccharide biosynthesis.<sup>4</sup> The quantifications were done using external calibration standards prepared from commercial samples (Figures S4 and S5).

Liquor samples were directly analyzed using both HPLC methods (pH 2 and pH 7 after neutralization with CaCO<sub>3</sub>) to quantify acids and monomeric sugars. To study the compositions of sugar oligomers, 100 mL of the un-neutralized sample was then acidified with 72% w/w H<sub>2</sub>SO<sub>4</sub> to achieve a final 4 wt% of H<sub>2</sub>SO<sub>4</sub> in the mixture. The exact loading of the 72% w/w sulfuric acid depended on the pH of the initial liquor, as specified in the NREL protocol.<sup>4</sup> The acidified liquor was digested at 120°C for 1 h in an autoclave to hydrolyze potential sugar oligomers. The hydrolysate was cooled, filtered, and analyzed with both HPLC methods again. The differences in the sugar monomer compositions before and after hydrolysis were assumed to be sugar oligomers. The measured quantities of sugar monomers were converted to those of the respective polysaccharides, accounting for the mass difference due to dehydration during polysaccharide biosynthesis.

Due to sugar degradation during acid hydrolysis, the sugar monomer yields after hydrolysis were corrected by a recovery factor for both solid and liquid samples.<sup>4</sup> The recovery factor was measured by digesting a known concentration of each sugar species with 4% H<sub>2</sub>SO<sub>4</sub> at 120°C for 1 h. The ratio of total detectable concentrations after

hydrolysis, accounting for possible degradation to furfural and 5-HMF, to the initial sugar concentration was used as the recovery factor.

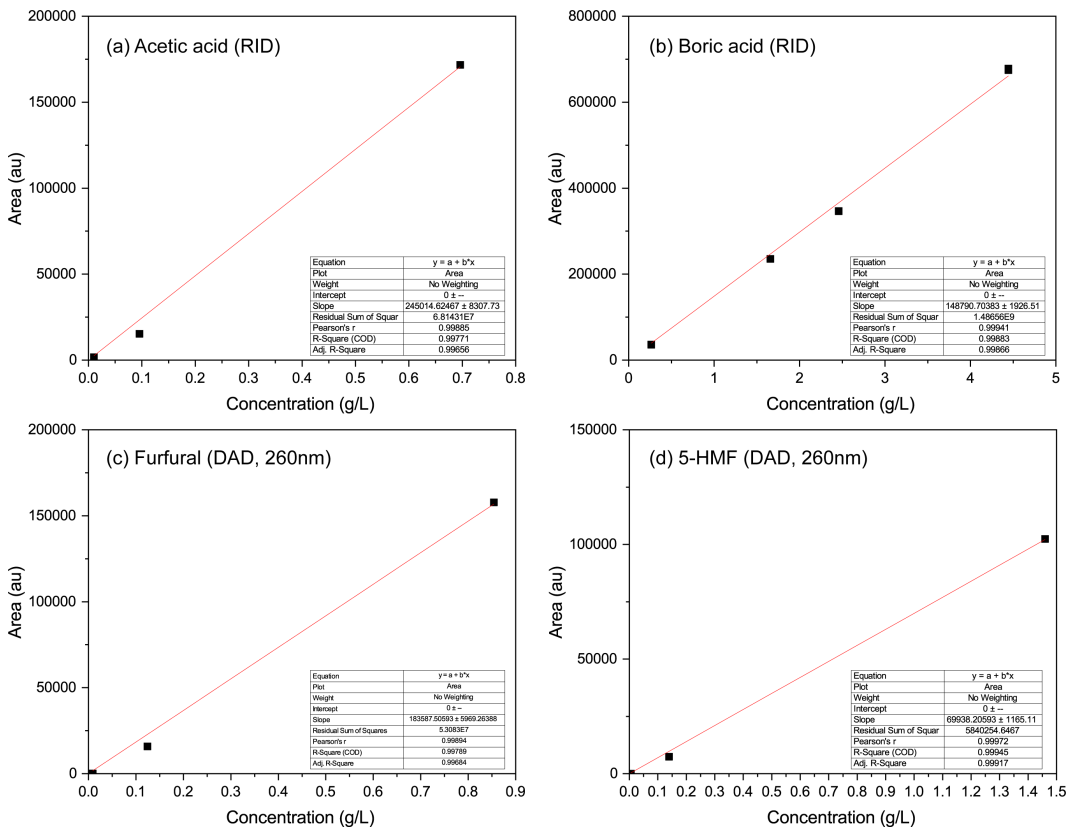


**Figure S4.** Calibration curve of (a) acetic acid, (b) boric acid, (c) furfural, and (d) 5-HMF using an HPLC with an Aminex HPX-87H Column and 0.05M H<sub>2</sub>SO<sub>4</sub> as the eluent.

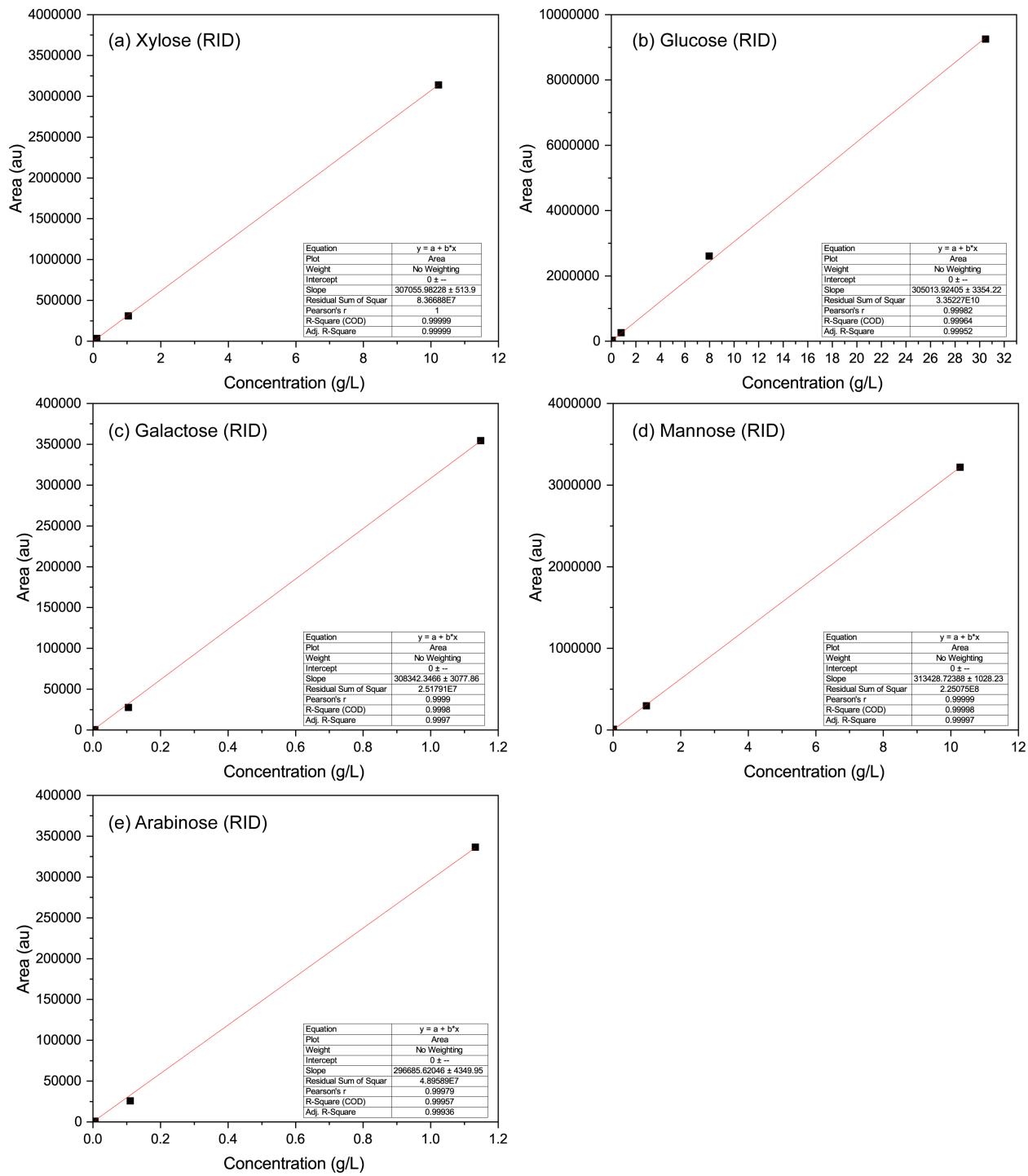


**Figure S5.** Calibration curve of (a) xylose, (b) glucose, (c) galactose, (d) mannose, and (e) arabinose using an HPLC with an Aminex HPX-87P Column and MQ water as the eluent.

### 3.2 Lignin monomer analysis by GC and GC-MS

Quantitative analysis of lignin monomer yield was performed with an Agilent 7890B series Gas Chromatography (GC) equipped with an HP5 column and a flame ionization detector (FID). The GC-FID method was performed as follows: The injection temperature was 300 °C. 1  $\mu$ L of the sample was injected with an autosampler in split mode (split ratio: 25:1). The column was initially kept at 40°C for 3 min, then was heated at a rate of 30°C/min to 100°C, followed by a heating rate of 40°C/min to 300°C that was held for 5 min. The monomer yield was calculated based on the effective carbon numbers (ECN) using n-decane as the internal standard.<sup>5-8</sup> This method has been validated in multiple studies from our group. The ECN values were retrieved from literature values.<sup>7,8</sup> Further discussion on quantification is detailed in Section 4.1.

Identification of monomer peaks in GC-FID chromatograms was performed using an Agilent 7890B series GC equipped with a HP5-MS capillary column and an Agilent 5977A series mass spectroscopy detector with electron ionization (EI). The peaks in the GC-MS chromatogram appear in the same order as those in the GC-FID chromatogram due to the use of a similar capillary column. The operating conditions were the same as GC-FID. Further discussion on peak identification is detailed in Section 4.1.

### 3.3 NMR analysis of lignin or lignin model compounds

NMR spectra (<sup>1</sup>H, <sup>13</sup>C, and <sup>1</sup>H-<sup>13</sup>C HSQC) were acquired using a Bruker Avance 500 MHz spectrometer (11.75 T) with a 5 mm proton-optimized triple resonance NMR ‘inverse’ TCI cryoprobe to reduce electronic noise and enhance acquisition sensitivity. Spectra were recorded using the standard pulse sequences from Bruker. Purity measurements were conducted by quantitative <sup>1</sup>H NMR with a recycle delay selected to be over 5 T1 using 1,2,4,5-Tetrachloro-3-nitrobenzene as the internal standard. <sup>11</sup>B NMR spectra were recorded using a Bruker Avance III 400 MHz spectrometer (T = 9.40 T) equipped with a BBFOz 5mm probe at an operating frequency of 96.294 MHz with a 90° pulse sequence and a recycle delay of 6 s, following the method by Aguilera-Sáez et al.<sup>9</sup> Quantitative measurements were conducted with 2,4,6-triphenylboroxin as the internal standard.

Quantitative <sup>31</sup>P NMR was performed following a procedure published by Meng et al.<sup>10</sup> Briefly, after drying the lignin samples in a vacuum oven at 50°C overnight, approximately 30 mg of lignin was dissolved with 0.5 mL of a pyridine-chloroform-d mixture (1.6:1 v/v). The mixture was stirred under Ar with a magnetic stir bar until fully dissolved. Quantitatively add 0.1mL of the internal standard solution (~5 mg/mL chromium(III) acetylacetone and ~18 mg/mL NHND in the same pyridine-chloroform-d mixture). Then, 0.1 mL of 2-chloro-4,4,5,5-tetramethyl-1,3-2-dioxaphospholane (TMDP) was added dropwise to the solution. The mixture was stirred for an additional hour at room temperature under Ar to achieve complete derivatization and then transferred to an NMR tube for measurement. The <sup>31</sup>P NMR spectra were recorded using a Bruker AvanceIII-HD 600 MHz spectrometer (14.10 T) with 5 mm BBO cryoprobe. The experimental parameters used for the spectra acquisition were: pulse program=inverse gated decoupling pulse (zgig), SW=395 ppm, O1P=140 ppm, AQ=0.34 s, D1=20 s, NS=64.

### **3.4 Pulp characterization**

#### **3.4.1 Kappa number titration**

The Kappa number of pulp samples was determined using manual titration, following the international standard ISO 302.<sup>11</sup> Briefly, a dispersed pulp suspension with a known mass of dry pulp was oxidized with potassium permanganate at 25°C for 10 min, during which time lignin and other oxidizable compounds in the pulp would reduce potassium permanganate to MnO<sub>2</sub>. The reaction was terminated by adding a known excess of KI solution, whereby the residual, unreacted permanganate oxidized iodide ions to elemental iodine. The formed iodine was then quantified using sodium thiosulfate titration. The consumption of sodium thiosulfate ultimately correlated with the quantity of reducing compounds, including lignin, in the pulp suspension. Numerically, the kappa number corresponds to the volume of 0.1 mol/L potassium permanganate (in mL) consumed by the oxidizable compounds in 1 gram of dry pulp.

#### **3.4.2 Schopper-Riegler number**

The Schopper-Riegler freeness test was conducted using an SR freeness tester (Frank-PTI), compliant with ISO 5267-1.<sup>12</sup> 1 L of a disintegrated pulp suspension of 0.2% consistency was added to the closed filling chamber. The sealing cone lifted to allow the suspension to drain through the screen, leaving a fibre pad, and the filtrate drained into the separating chamber. The water volume fraction drained through the side discharge pipe was weighed. The °SR corresponds to the volume of the water exiting the separating chamber through the bottom capillary discharge. A lower °SR means faster water drainage. Note that the Canadian Standard Freeness is another standard way to measure water drainage rate. Although it was not used in this study, it is worth mentioning to avoid confusion, since it has an inverted scale, where a higher value means faster drainage.

#### **3.4.3 Size analysis**

The mean pulp fibre length and width were measured using a Fibre Quality Analyzer (OpTest Equipment), fully compliant with TAPPI T 271.<sup>13</sup> Fibres were continuously fed into a flow cell and imaged under a polarized light source. The average dimensions were automatically processed and reported by integrated image analysis.

#### **3.4.4 Optical microscopy**

The pulp fibres were visually examined with an optical microscope equipped with a polarized light source (Nikon Eclipse LV100N POL). The 0.3% pulp suspension was diluted 3-5 times before loading onto the glass slide.

### **3.5 Handsheet characterization**

#### **3.5.1 Brightness**

The handsheet brightness was measured with a spectrophotometer (CM-2500d, Minolta, Japan), according to ISO 2470-1.<sup>14</sup> This ISO brightness corresponds to the diffuse reflectance of blue light at a wavelength of 457 nm, measured under a D65 light source (daylight equivalent), using a 10° standard observer. All measurements were performed on

conditioned handsheets ( $23 \pm 1$  °C,  $50 \pm 2$  % relative humidity), and the reported brightness values correspond to the mean of at least 5 replicates per sample.

### 3.5.2 Thickness

The thickness of the handsheet was measured using an automated micro calliper (L&W). Eight sampling locations were evenly selected on each handsheet and the average and the standard deviation were used in reporting.

### 3.5.4 Tensile index

The tensile index was measured using a L&W Tensile Strength Tester based on Tappi T 494.<sup>15</sup> Handsheets were left in the climate-controlled room (50% RH and 23°C) to equilibrate overnight. They were cut into testing strips 15 mm wide with a minimum of 100 mm in length and loaded onto the tester. The tensile strength was measured automatically. Four replicates were measured for each pulp type. The tensile index and the breaking length were calculated based on the measured grammage and thickness using the following equations. Breaking length corresponds to the maximum length of a paper sheet before it breaks under its own weight when suspended vertically.

$$\text{Tensile index} = \frac{\text{tensile strength}}{\text{grammage}} = \frac{F_{\max,\text{tensile}}}{\text{strip width} \times \text{grammage}} \quad \text{S1}$$

$$\text{Breaking length} = \frac{F_{\max,\text{tensile}}}{\text{strip width} \times \text{grammage} \times \text{gravitational acceleration}} \quad \text{S2}$$

### 3.5.5 Optical microscopy

The surface morphology of the handsheets was examined using a stereomicroscope (Stemi SV 11, Zeiss, Germany) equipped with Zeiss Plan S 1.0x objective and additional lateral LQ LED M illumination (Fiberoptic-Heim AG, Germany).

## 4. Supporting results and discussion

### 4.1 Lignin monomer identification and quantification

#### 4.1.1 Monomer identification

Most lignin monomers after hydrogenolysis have been identified in the previous studies from our group.<sup>5-8</sup> In these studies, GC-MS was used to identify the mass fragments and compare them with the purchased or synthesized standards. In this study, we also confirmed the monomers produced from BAF lignin hydrogenolysis using GC-MS mass fragments and verified the identification with literature results.<sup>5</sup> Although the retention time of the same compound was not identical in GC-MS and GC-FID due to the inherent instrumental differences, the peaks appeared in the same order, so we could identify the GC-FID peaks. Example GC-MS and GC-FID chromatograms are compared in Figure S6 with the monomer structure labelled to each peak. Figure S7 further shows the mass spectrum of each identified peak and the possible fragmentation modes that produced major mass fragments.

Compared to prior reports of lignin hydrogenolysis monomers,<sup>5,7</sup> O-demethylated products (M3' and M7') were detected in this work, likely due to the co-presence of water and HCl during hydrogenolysis. Lignin was dissolved from the lignin-xylan mixture after HCl acidification to precipitate lignin and xylan, as detailed in Section 2.2.1.1. The co-precipitate was not thoroughly dried to avoid condensation. Therefore, water and HCl propagated into the hydrogenolysis mixture, which could lead to O-demethylation of lignin monomers, according to many literature reports reviewed by Wu *et al.*<sup>16</sup>

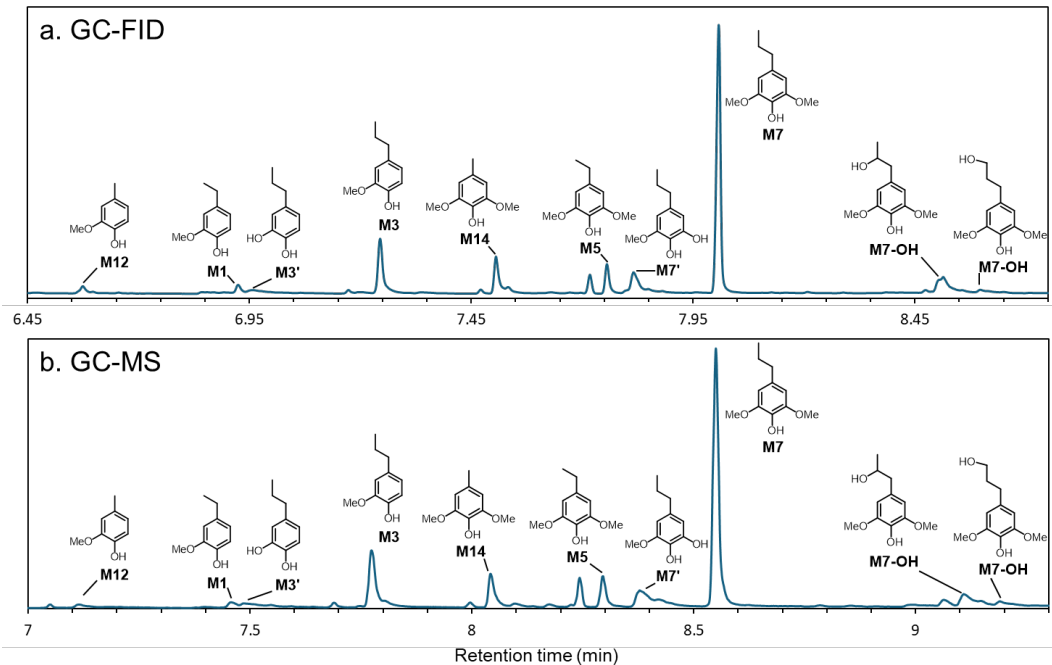


**Figure S6.** Gas chromatogram comparison of the same hydrogenolysis liquor of beech lignin extracted with boric acid at 150°C for 1.5 h (a) GC-FID and (b) GC-MS, showing identified monomers.

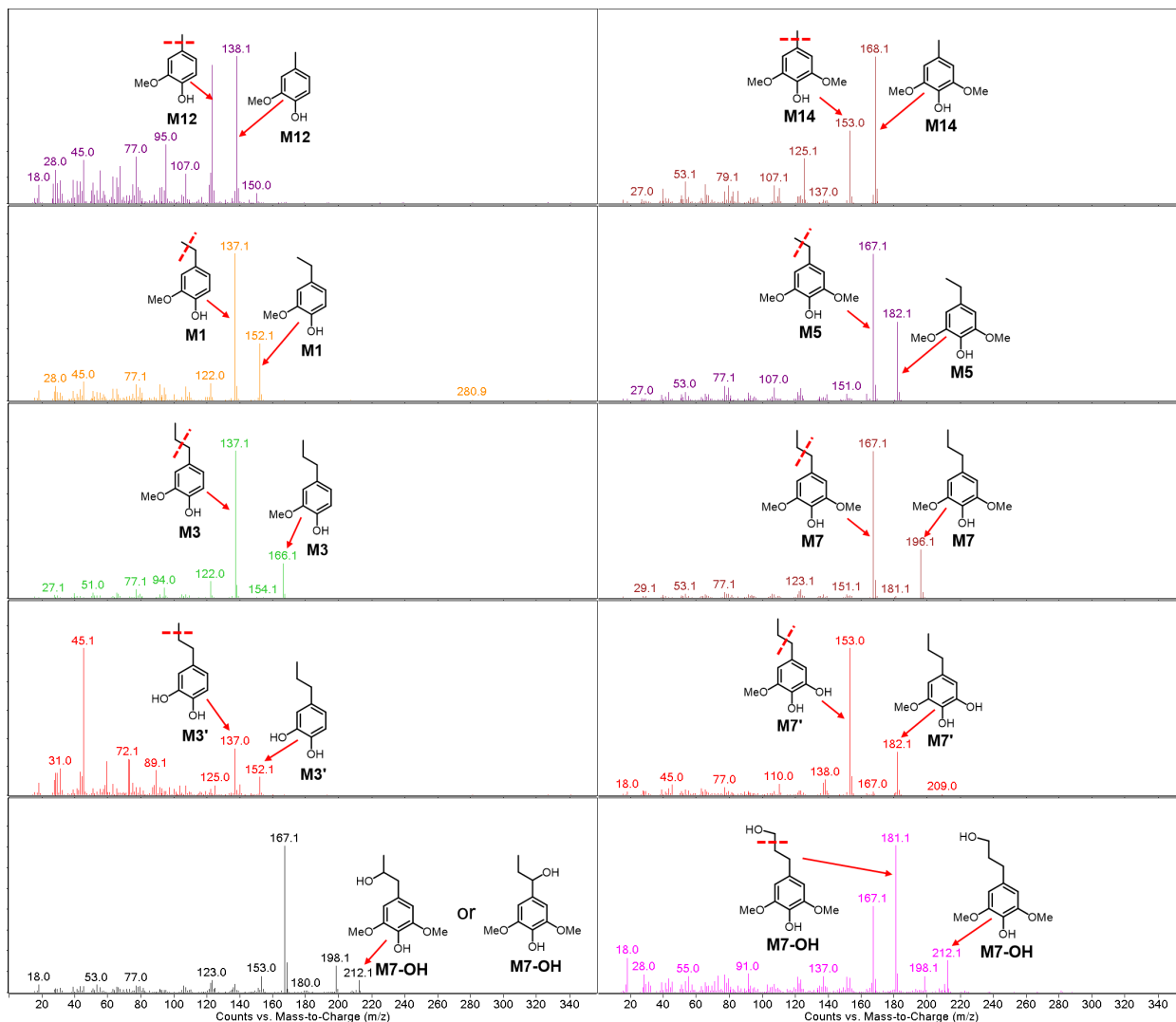


**Figure S7.** GC-MS spectra of identified lignin monomers and possible modes of fragmentation. The molecular ion and major fragment are highlighted.

#### 4.1.2 Monomer quantification

Due to the difficulty in obtaining a large quantity of purified lignin monomers as external calibration standards, we calculated their yields with effective carbon numbers (ECNs) using n-decane as the internal standard. The ECNs of these compounds have been calculated and verified using isolated compounds in previous studies.<sup>3,5,7</sup> The values used in this study are summarized in Table S2. Yields were calculated based on Klason lignin and did not include acid-soluble lignin (ASL), as is consistent with the vast majority of previously reported lignin yields. This is suitable in this study since lignin precipitation was realized by acidification. ASL was assumed not to precipitate, remaining in the liquor. Lignin monomers originally exist in lignin as phenylpropanoids, while structural alterations occurred during hydrogenolysis. To reflect its original structure, the yield of each monomer was converted to its corresponding phenylpropanoid subunit (i.e., the coniferyl or sinapyl unit, the mass of which is also listed in Table S2) in line with standard guidelines.<sup>17</sup>

As mentioned above and compared to lignin monomers produced in RCF, the hydrogenolysis of BAF lignin produced demethylated monomers, which were not previously observed when using AAF lignin. This likely resulted from the use of a small amount of HCl during BAF lignin hydrogenolysis. The intention was to remove the BA species from lignin ether linkages through hydrolysis and to ensure that the BA protection did not interfere with ether bond cleavage. In practice, HCl was proven to catalyze the cleavage of methyl aryl ethers and was often used as a modification method to increase the hydroxyl content in technical lignin and lignin monomers after hydrogenolysis.<sup>18,19</sup> Although water was not intentionally added during BAF lignin hydrogenolysis, it was introduced with the lignin solution, as lignin was dissolved from the mixed precipitate without thorough drying. The existence of water and HCl constitutes the conditions in which cleavage of methyl aryl ethers might occur.<sup>18,19</sup> The syringyl alcohol yield from BAF lignin hydrogenolysis was also higher than that of RCF lignin, which may also be related to the presence of HCl. Literature reported higher yields of monomers with hydroxyl groups on the side chain when RCF was conducted with HCl.<sup>20</sup> From the mass fragments in GC-MS, there may be more than one type of syringyl alcohol produced (Figure S7). The exact location of the hydroxyl group on the side chain was not distinguished in this study for quantification, as the ECNs of these species were expected to be similar. A combined yield of these isomers is reported in this work. The role of boron species during hydrogenolysis may be investigated in the future. It has been proposed that boric and boronic acids may act as Lewis acids, which are known to be involved in lignin ether cleavage, demethylation, and alkene hydration reactions.<sup>21</sup>

**Table S2.** The effective carbon numbers for lignin monomers.

Compounds	ECN	Molecular weight (g/mol)	Original molecular weight in lignin (g/mol)
<b>n-decane (internal standard)</b>	10	142.29	142.29
<b>M12</b>	7.19	138.07	196.20
<b>M1</b>	8.19	152.08	196.20
<b>M3</b>	9.02	166.10	196.20
<b>M3'</b>	8.02	152.08	196.20
<b>M14</b>	6.06	168.08	226.23
<b>M5</b>	7.06	182.09	226.23
<b>M7</b>	7.78	196.11	226.23
<b>M7'</b>	6.78	182.09	226.23
<b>M7-OH</b>	6.78	212.10	226.23

## 4.2 Fractionation and condition optimization in the 100 mL reactor

### 4.2.1 Additional HSQC spectra

To confirm the reaction between the diol motif in the  $\beta$ -O-4 linkage and boric or boronic acid species, a series of comparisons was made using the  $^1\text{H}$ - $^{13}\text{C}$  HSQC NMR spectra of model compounds and birch extracts with and without the BA protection. Without further purification, almost all VG dimers were protected with phenylboronic acid in dioxane after 1 h of reaction. The cross peaks corresponding to the unprotected  $\beta$ -O-4 linkage were barely visible (Figure S7a-b). However, using the same reaction conditions with wood chips proved unsuccessful,<sup>7</sup> likely because of the low solubility of xylan in dioxane. Although BA-protected lignin, like the protected VG dimer, was soluble in dioxane, xylan was not. If xylan could not be effectively extracted from the wood matrix, lignin would likely be trapped inside the lignin-carbohydrate complex, so it could not be extracted efficiently, either. Therefore, it is imperative to use a solvent in which all extracted fractions have high solubility. Concentrated NaOH solution was used in this study due to its longstanding use in the pulp industry, which has proven its excellent ability to solubilize both lignin and xylan.<sup>22</sup>

Lignin peaks were assigned according to our previous work,<sup>5</sup> while xylan peaks were assigned with external literature values.<sup>23</sup> Compared to other lignin fractions, the lignin extracted without BA protection (Figure S8d) showed the characteristic cross peaks corresponding to condensed syringyl units,<sup>24</sup> while lignin extracted with protection (Figure S8e-f) did not show significant condensation peaks. We further compared the extracted lignin structures with the mild acidolysis lignin extracted from the same batch of birch chips (Figure S8c). Mild acidolysis lignin showed no NMR peaks related to hemicellulose, likely because acid hydrolysis effectively converted hemicellulose to sugar monomers.

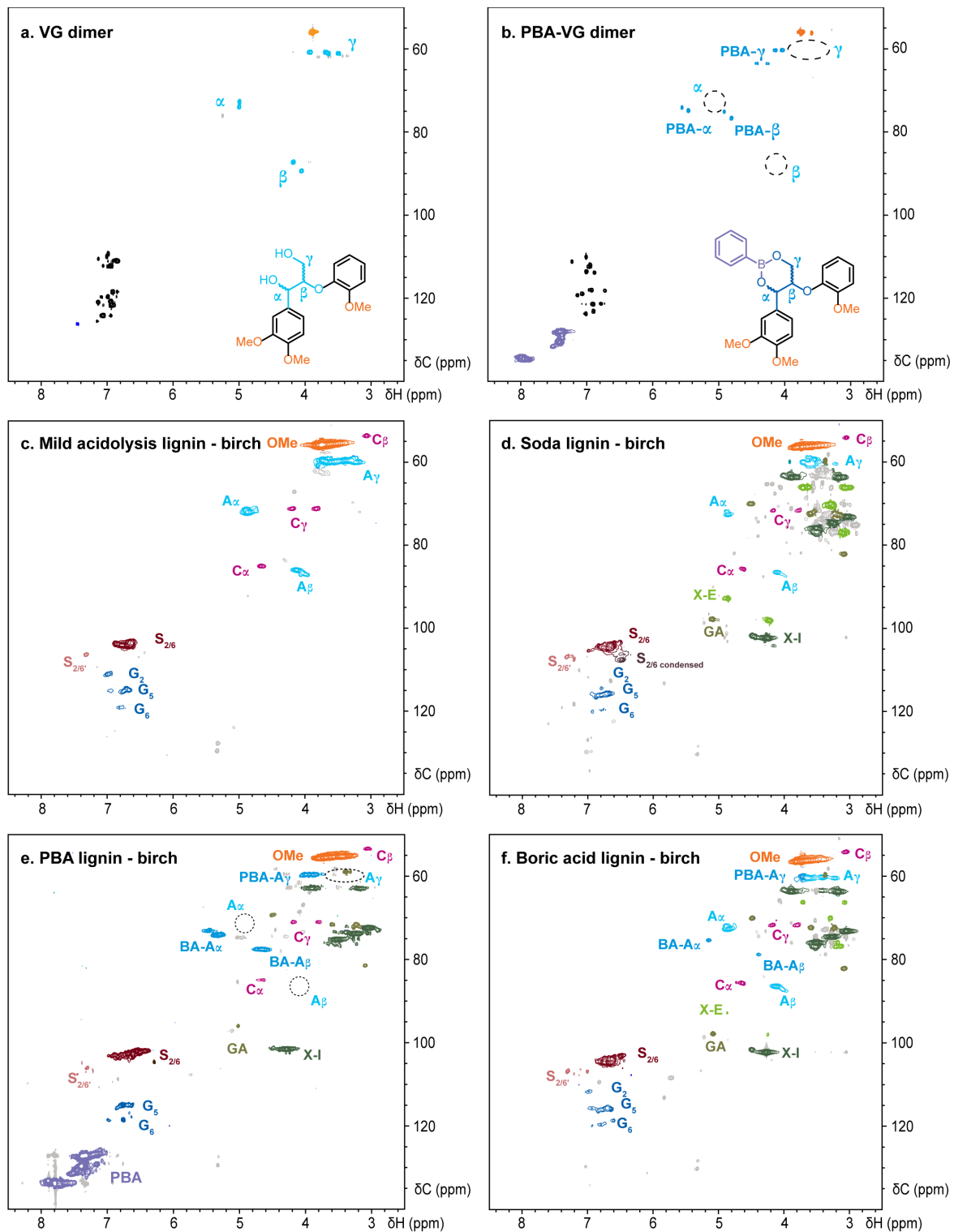


**Figure S8.**  $^1\text{H}$ - $^{13}\text{C}$  HSQC NMR spectra of (a) veratrylglycerol-  $\beta$ -guaiacyl ether (VG dimer) (b) VG dimer with phenylboronic acid protection, (c) mild acidolysis lignin extracted from birch, and the extracted lignin and xylan from birch (d) without protection, (e) with phenylboronic acid and (f) boric acid as the protecting agent. (130°C, 1M NaOH, 1.5 h). Panels (b), (e), and (f) are presented in Figure 1 in the main text with adaptation. X-E: end unit of xylan, X-I: internal unit of xylan, GA: 4-O-methyl- $\alpha$ -D-glucuronic acid.

#### 4.2.2 Tabulated lignin monomer yields

The hydrogenolysis monomer yields of extracted lignin and direct hydrogenolysis on wood chips are tabulated in this section. Particularly, the monomer yields of lignin extracted from sequential fractionation were reported in plots as the sum of the monomer yields of lignin fractions from all stages. The monomer yields from the individual lignin fractions are shown in Tables S3-S7. The yield is reported based on the total dry loading of wood.

**Table S3.** Lignin monomer yields in single pass BA screening (plotted in Figure 2a).

Entry	BA species	Lignin monomer yield % (dry wood-basis)										Delignification efficiency (%)
		M12	M1	M3	M3'	M14	M5	M7	M7'	M7-OH	Others	
1	Boric acid	0.03	0.03	0.19	0.05	0.07	0.05	1.04	0.24	0.05	0.03	26.5
2	Methyl-BA	0.05	0.05	0.25	0.03	0.12	0.10	1.47	0.19	0.03	0.02	33.4
3	Propyl-BA	0.04	0.04	0.20	0.03	0.10	0.09	1.23	0.15	0.03	0.03	32.0
4	Butyl-BA	0.03	0.04	0.19	0.02	0.08	0.08	1.07	0.11	0.02	0.01	33.5
5	Phenyl-BA	0.05	0.03	0.29	0.15	0.12	0.09	1.52	0.08	0.15	0.01	26.9
6	Soda control	0.04	0.03	0.10	0.01	0.07	0.09	0.50	0.04	0.01	0.00	34.6

**Table S4.** Hydrogenolysis monomer yields of lignin extracted in 3 full sequential BAF configurations (The total yields were plotted in Figure 2c).

Entry	Temp. stage	Lignin monomer yield % (dry wood-basis)										Delignification efficiency (%)
		M12	M1	M3	M3'	M14	M5	M7	M7'	M7-OH	Others	
<b>Cross-current Birch fractionation with phenylboronic acid protection</b>												
1	130°C	0.05	0.03	0.31	0.17	0.14	0.09	1.53	0.07	0.05	0.02	-
2	150°C	0.07	0.04	0.31	0.10	0.29	0.16	1.20	0.05	0.01	0.02	-
3	170°C	0.07	0.04	0.22	0.06	0.18	0.09	0.51	0.03	0.01	0.02	-
4	180°C	0.03	0.01	0.10	0.03	0.05	0.02	0.12	0.01	0.00	0.01	-
	Sum	0.22	0.11	0.95	0.36	0.65	0.36	3.36	0.15	0.07	0.06	96.79
<b>Repeat</b>												
5	130°C	0.05	0.03	0.27	0.13	0.10	0.08	1.51	0.10	0.04	0.01	-
6	150°C	0.07	0.05	0.29	0.10	0.26	0.16	1.18	0.04	0.02	0.02	-
7	170°C	0.06	0.04	0.24	0.05	0.14	0.08	0.55	0.03	0.01	0.01	-
8	180°C	0.03	0.01	0.10	0.02	0.05	0.02	0.14	0.01	0.00	0.01	-
	Sum	0.22	0.13	0.89	0.31	0.55	0.34	3.39	0.17	0.07	0.05	97.70

<b><u>Cross-current Birch fractionation with boric acid protection</u></b>												
<b>9</b>	130°C	0.04	0.04	0.19	0.04	0.06	0.05	1.08	0.22	0.15	0.01	-
<b>10</b>	150°C	0.06	0.04	0.26	0.09	0.26	0.13	0.99	0.30	0.31	0.05	-
<b>11</b>	170°C	0.03	0.03	0.18	0.03	0.12	0.05	0.43	0.13	0.07	0.01	-
<b>12</b>	180°C	0.04	0.00	0.08	0.02	0.05	0.03	0.12	0.06	0.03	0.01	-
	Sum	0.17	0.13	0.71	0.19	0.49	0.26	2.62	0.71	0.55	0.08	97.21
<b>Repeat</b>												
<b>13</b>	130°C	0.05	0.04	0.20	0.06	0.07	0.06	1.04	0.22	0.08	0.01	-
<b>14</b>	150°C	0.07	0.05	0.32	0.11	0.28	0.13	1.01	0.32	0.29	0.02	-
<b>15</b>	170°C	0.04	0.04	0.19	0.02	0.12	0.05	0.44	0.10	0.05	0.01	-
<b>16</b>	180°C	0.03	0.01	0.07	0.02	0.05	0.03	0.12	0.05	0.01	0.00	-
	Sum	0.19	0.15	0.78	0.22	0.52	0.26	2.60	0.69	0.44	0.05	97.07
<b><u>Cross-current Birch fractionation without BA protection (i.e., Soda control)</u></b>												
<b>17</b>	130°C	0.04	0.03	0.10	0.01	0.07	0.09	0.48	0.04	0.00	0.00	-
<b>18</b>	150°C	0.02	0.04	0.12	0.01	0.16	0.17	0.51	0.05	0.00	0.01	-
<b>19</b>	170°C	0.02	0.03	0.08	0.00	0.06	0.07	0.23	0.01	0.00	0.00	-
<b>20</b>	180°C	0.01	0.01	0.02	0.00	0.01	0.02	0.05	0.01	0.00	0.00	-
	Sum	0.08	0.10	0.31	0.02	0.29	0.35	1.26	0.11	0.00	0.01	95.38
<b>Repeat</b>												
<b>21</b>	130°C	0.04	0.03	0.08	0.01	0.06	0.08	0.46	0.04	0.00	0.00	-
<b>22</b>	150°C	0.03	0.04	0.13	0.01	0.17	0.17	0.50	0.05	0.00	0.01	-
<b>23</b>	170°C	0.02	0.03	0.08	0.00	0.06	0.07	0.22	0.01	0.00	0.00	-
<b>24</b>	180°C	0.01	0.01	0.02	0.00	0.01	0.02	0.04	0.01	0.00	0.00	-
	Sum	0.09	0.10	0.31	0.02	0.30	0.35	1.23	0.11	0.00	0.01	95.27
<b><u>Mixed-current Birch fractionation with boric acid protection</u></b>												
<b>25</b>	130°C	0.05	0.03	0.23	0.06	0.09	0.06	0.97	0.12	0.12	0.03	-
<b>26</b>	150°C	0.10	0.10	0.46	0.08	0.40	0.17	1.52	0.47	0.53	0.04	-
	180°C											
	Sum	0.15	0.13	0.69	0.14	0.49	0.23	2.49	0.59	0.65	0.07	99.24
<b>Repeat</b>												
<b>27</b>	130°C	0.04	0.03	0.21	0.07	0.08	0.06	1.02	0.14	0.08	0.02	-
<b>28</b>	150°C	0.11	0.11	0.45	0.08	0.38	0.16	1.52	0.55	0.44	0.02	-
	180°C											
	Sum	0.15	0.14	0.66	0.15	0.46	0.22	2.54	0.69	0.52	0.04	98.60
<b><u>Mixed-current Birch fractionation without BA protection (i.e., Soda control)</u></b>												
<b>29</b>	130°C	0.03	0.02	0.08	0.03	0.07	0.07	0.35	0.03	0.03	0.01	-

<b>30</b>	150°C	0.05	0.07	0.18	0.00	0.27	0.27	0.75	0.09	0.10	0.01	-
	-											
	180°C											
	Sum	0.09	0.09	0.26	0.03	0.34	0.34	1.10	0.12	0.13	0.02	98.69
<b>Repeat</b>												
<b>31</b>	130°C	0.03	0.02	0.06	0.01	0.06	0.09	0.34	0.05	0.03	0.00	-
<b>32</b>	150°C	0.05	0.08	0.19	0.00	0.24	0.21	0.72	0.07	0.07	0.01	-
	-											
	180°C											
	Sum	0.08	0.09	0.26	0.01	0.31	0.30	1.06	0.11	0.10	0.02	98.36
<b>Counter-current Birch fractionation with boric acid protection</b>												
<b>33</b>	All	0.10	0.12	0.51	0.13	0.51	0.44	2.17	0.24	0.30	0.02	97.89
<b>Repeat</b>												
<b>34</b>	All	0.12	0.12	0.58	0.14	0.41	0.25	2.18	0.42	0.40	0.07	97.38
<b>Counter-current Birch fractionation without BA protection (i.e., Soda control)</b>												
<b>35</b>	All	0.06	0.11	0.24	0.01	0.30	0.31	1.02	0.12	0.00	0.01	98.23
<b>Repeat</b>												
<b>36</b>	All	0.04	0.10	0.27	0.01	0.29	0.30	1.02	0.09	0.03	0.01	98.39

\* All experiments in Table S4 were conducted in duplicates.

**Table S5.** Hydrogenolysis monomer yields of lignin extracted from different wood species (The total yields were plotted in Figure 2d).

Entry	Temp.	Lignin monomer yield % (dry wood-basis)									Delignification efficiency (%)	
		stage	M12	M1	M3	M3'	M14	M5	M7	M7'		
<b>Cross-current Birch fractionation with boric acid protection (average of entry 9-16 in Table S4)</b>												
<b>1</b>	130°C	0.05	0.04	0.20	0.05	0.07	0.06	1.06	0.22	0.12	0.01	-
<b>2</b>	150°C	0.07	0.05	0.29	0.10	0.27	0.13	1.00	0.31	0.30	0.04	-
<b>3</b>	170°C	0.04	0.04	0.19	0.03	0.12	0.05	0.44	0.12	0.06	0.01	-
<b>4</b>	180°C	0.04	0.01	0.08	0.02	0.05	0.03	0.12	0.06	0.02	0.01	-
	Sum	0.18	0.14	0.75	0.21	0.51	0.26	2.61	0.70	0.50	0.07	97.15
<b>5</b>	RCF	0.12	1.39	0.31	0.00	0.41	6.04	0.97	0.00	0.08	0.02	-*
<b>Cross-current Beech fractionation with boric acid protection</b>												
<b>6</b>	130°C	0.06	0.10	0.51	0.01	0.09	0.11	1.25	0.09	0.09	0.01	-
<b>7</b>	150°C	0.04	0.09	0.34	0.01	0.26	0.15	0.94	0.08	0.15	0.01	-
<b>8</b>	170°C	0.02	0.04	0.11	0.00	0.09	0.07	0.30	0.01	0.02	0.01	-
<b>9</b>	180°C	0.01	0.03	0.06	0.00	0.03	0.02	0.08	0.00	0.01	0.00	-
	Sum	0.13	0.25	1.02	0.02	0.46	0.35	2.57	0.18	0.26	0.03	97.93
<b>10</b>	RCF	0.18	1.77	0.53	0.00	0.46	4.15	0.82	0.00	0.00	0.09	-*

<b>Cross-current Pine fractionation with boric acid protection</b>												
<b>11</b>	130°C	0.10	0.13	0.53	0.03	0.00	0.00	0.00	0.00	0.00	0.00	-
<b>12</b>	150°C	0.04	0.08	0.27	0.00	0.00	0.00	0.00	0.00	0.00	0.00	-
<b>13</b>	170°C	0.03	0.06	0.19	0.01	0.00	0.00	0.00	0.00	0.00	0.00	-
<b>14</b>	180°C	0.15	0.18	0.43	0.01	0.00	0.00	0.00	0.00	0.00	0.00	-
	Sum	0.32	0.46	1.42	0.05	0.00	0.00	0.00	0.00	0.00	0.00	85.85
<b>15</b>	RCF	0.32	1.86	0.47	0.00	0.00	0.00	0.00	0.00	0.00	0.00	-*

<b>Cross-current Spruce fractionation with boric acid protection</b>												
<b>16</b>	130°C	0.08	0.09	0.45	0.02	0.00	0.00	0.00	0.00	0.00	0.00	-
<b>17</b>	150°C	0.07	0.06	0.27	0.04	0.00	0.00	0.00	0.00	0.00	0.00	-
<b>18</b>	170°C	0.07	0.08	0.25	0.00	0.00	0.00	0.00	0.00	0.00	0.00	-
<b>19</b>	180°C	0.15	0.13	0.34	0.00	0.00	0.00	0.00	0.00	0.00	0.00	-
	Sum	0.36	0.35	1.31	0.05	0.00	0.00	0.00	0.00	0.00	0.00	84.71
<b>20</b>	RCF	0.30	2.31	0.56	0.00	0.00	0.00	0.00	0.00	0.00	0.00	-*

\*Not experimentally measured.

**Table S6.** Lignin monomer yields in the cross-current condition optimization (plotted in Figure S10).

Entry	Stage	Lignin monomer yield % (dry wood-basis)										Delignification efficiency (%)
		M12	M1	M3	M3'	M14	M5	M7	M7'	M7-OH	Others	
<b>Stage 1: 130°C, birch with phenylboronic acid protection</b>												
<b>1</b>	130°C 1 h	0.02	0.09	0.17	0.00	0.15	0.67	1.25	0.00	0.00	0.10	28.41
<b>2</b>	130°C 2 h	0.07	0.31	0.11	0.00	0.41	1.86	0.36	0.00	0.00	0.18	36.51
<b>3</b>	130°C 3 h	0.06	0.22	0.16	0.00	0.54	1.58	0.78	0.00	0.00	0.19	42.06
<b>4</b>	130°C 4 h	0.06	0.27	0.13	0.00	0.60	1.76	0.50	0.00	0.00	0.24	45.13
<b>5</b>	130°C 6 h	0.09	0.23	0.19	0.00	0.76	1.02	0.93	0.00	0.00	0.10	51.24
<b>Stage 2: 150°C, after 130°C for 2 h birch with phenylboronic acid protection</b>												
<b>6-1</b>	130°C 2 h	0.02	0.15	0.10	1.00	0.28	1.48	0.60	0.00	0.00	0.22	36.51 <sup>[a]</sup>
<b>6-2</b>	150°C 0.75 h	0.05	0.16	0.06	6.00	0.37	0.90	0.21	0.00	0.00	0.07	25.72 <sup>[b]</sup>
<b>7-1</b>	130°C 2 h	0.03	0.19	0.13	2.00	0.29	1.54	0.70	0.00	0.00	0.17	36.51 <sup>[a]</sup>
<b>7-2</b>	150°C 1 h	0.07	0.22	0.08	7.00	0.52	1.06	0.29	0.00	0.00	0.06	29.94 <sup>[b]</sup>
<b>8-1</b>	130°C 2 h	0.06	0.24	0.15	3.00	0.44	1.77	0.78	0.00	0.00	0.18	36.51 <sup>[a]</sup>
<b>8-2</b>	150°C 1.5 h	0.09	0.22	0.07	8.00	0.55	1.01	0.19	0.00	0.00	0.04	33.82 <sup>[b]</sup>

<b>9-1</b>	130°C 2 h	0.08	0.23	0.17	4.00	0.46	1.49	0.86	0.00	0.00	0.12	36.51 <sup>[a]</sup>
<b>9-2</b>	150°C 2 h	0.05	0.16	0.05	9.00	0.39	0.82	0.15	0.00	0.00	0.07	33.91 <sup>[b]</sup>
<b>Stage 3: 170°C, after 130°C for 2 h and 130°C for 1.5 h birch with phenylboronic acid protection</b>												
<b>10-1</b>	130°C 2 h	0.08	0.26	0.14	1.00	0.42	1.70	0.61	0.00	0.00	0.14	36.51 <sup>[a]</sup>
<b>10-2</b>	150°C 1.5 h	0.04	0.11	0.03	4.00	0.19	0.56	0.09	0.00	0.00	0.10	33.82 <sup>[b]</sup>
<b>10-3</b>	170°C 0.25 h	0.04	0.10	0.05	7.00	0.19	0.36	0.09	0.00	0.00	0.02	10.58 <sup>[c]</sup>
<b>11-1</b>	130°C 2 h	0.03	0.17	0.11	2.00	0.27	1.37	0.62	0.00	0.00	0.19	36.51 <sup>[a]</sup>
<b>11-2</b>	150°C 1.5 h	0.03	0.10	0.04	5.00	0.21	0.54	0.10	0.00	0.00	0.08	33.82 <sup>[b]</sup>
<b>11-3</b>	170°C 0.5 h	0.03	0.08	0.04	8.00	0.15	0.28	0.06	0.00	0.00	0.02	19.15 <sup>[c]</sup>
<b>12-1</b>	130°C 2 h	0.05	0.17	0.11	3.00	0.40	1.50	0.65	0.00	0.00	0.15	36.51 <sup>[a]</sup>
<b>12-2</b>	150°C 1.5 h	0.04	0.13	0.05	6.00	0.31	0.74	0.15	0.00	0.00	0.05	33.82 <sup>[b]</sup>
<b>12-3</b>	170°C 0.75 h	0.03	0.07	0.03	9.00	0.12	0.20	0.05	0.00	0.00	0.00	22.69 <sup>[c]</sup>

<sup>[a]</sup> Delignification efficiency was assumed to be the same as the single-stage fractionation under the same condition in entry 2. <sup>[b]</sup> The value was estimated based on the total delignification efficiency after both stages subtracted by the delignification extent in the first stage in entry 2. <sup>[c]</sup> The value was estimated based on the total delignification efficiency after three stages subtracted by the delignification extent in the first two stages in entries 8-1 and 8-2.

#### 4.2.3 Effect of electrophilicity on protection efficiency

There was a strongly negative correlation between lignin monomer yield based on the extracted Klason lignin and the pKa of the boric or boronic acid used as the protecting agent. A Spearman's correlation test was conducted to evaluate the statistical significance (summarized in Table S7). This correlation was highlighted with a Spearman's coefficient of -1 and a p-value of  $4 \times 10^{-24}$ .

The lignin monomer yield based on the extracted Klason lignin indicates the effectiveness of the protection. BA is a Lewis acid. A higher pKa means a lower electrophilicity of the boron atom in the BA species.<sup>25</sup> Therefore, as the electrophilicity of the boron decreased, it would be less prone to a nucleophilic attack from the hydroxyl group, which is the initial step of boric or boronic ester formation.<sup>25</sup>

**Table S7.** Spearman's correlation statistics.

	Values
<b>Spearman's Correlation Coefficient, <math>r_s</math></b>	-1.0
<b>Degree of Freedom</b>	3
<b>P Value</b>	$3.97 \times 10^{-24}$

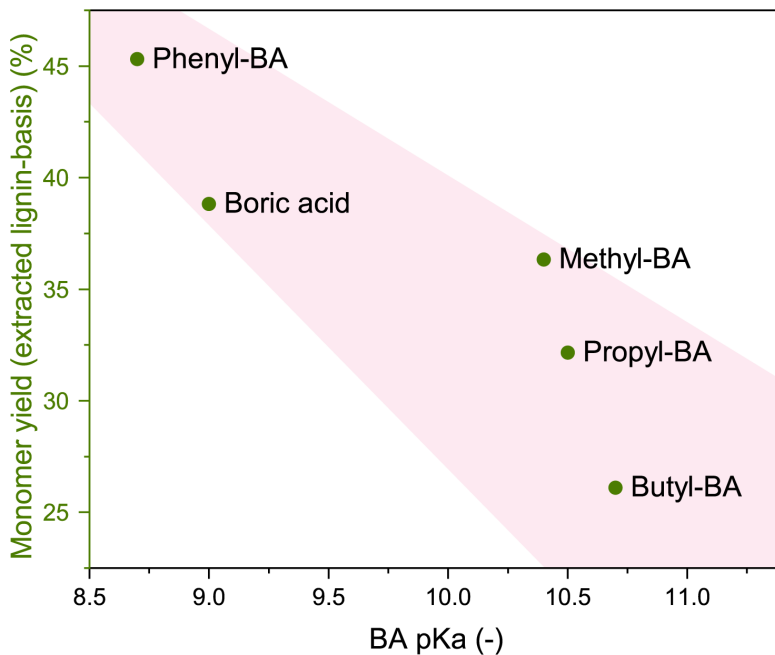


**Figure S9.** The effect of pKa of the boric or boronic acid as the lignin protection group on the lignin monomer yield after hydrogenolysis. The pKa values were retrieved from literature.<sup>25</sup>

#### 4.2.4 Sequential optimization

The fractionation duration at each temperature stage was selected based on the optimization conducted on the cross-current configuration with phenylboronic acid protection. Without further adjustment, the same conditions at each temperature were used for mixed- and counter-current systems and with different BA species. During the optimization stage, the trade-off between delignification efficiency and the lignin degradation extent was to be balanced. The optimization started with the first BAF stage at 130°C. The digestion time varied between 1 h and 6 h. Monomer yields were measured after the hydrogenolysis of the extracted lignin, and the delignification efficiency was calculated based on the remaining Klason lignin in the cellulose-rich fraction. Hence, the lignin monomer yield based on the extracted Klason lignin could be calculated and used as the indicator of the protection effectiveness (Figure S10a). After the initial 2 h, the extracted lignin started to degrade despite the phenylboronic acid protection. The delignification extent also showed a diminishing return after extending the digestion time over 3 h. Therefore, the digestion time at 130°C was tentatively selected to be 2 h for the optimization of the following stages. The same experiments were conducted at 150°C after treating all wood chips at 130°C for 2 h. Limited by the small amount of wood used (3 g) during optimization, it was impractical to divert a part of the solid to measure the residual lignin content between fractionation stages. The values measured at the end of a previous optimization stage under the same conditions were assumed. For example, a total delignification efficiency of 62.2% was measured after two consecutive fractionation stages at 130°C for 2 h and 150°C for 0.75 h. The 130°C stage removed 36.5% Klason lignin during the optimization of the 130°C stage. Assuming that value was repeatable, the remainder of 25.7% should be removed at the 150°C stage. Although stage-wise lignin removal was only calculated, hydrogenolysis monomer yield was directly measured stage by stage. Therefore, the protection effectiveness can be estimated for each stage (green dots in Figure S10). Lignin degradation accelerated after 2 h at 130°C, after 1 h at 150°C and only after 15 min at 170°C. As the fractionation temperature

increased, the time window in which the extracted lignin remained uncondensed clearly narrowed. Therefore, the fractionation time at each temperature stage had to be carefully decided. As proof of concept, the conditions used in this work were not optimized for each configuration and wood-BA pair. However, they may be systematically optimized in the future to assist detailed process development.

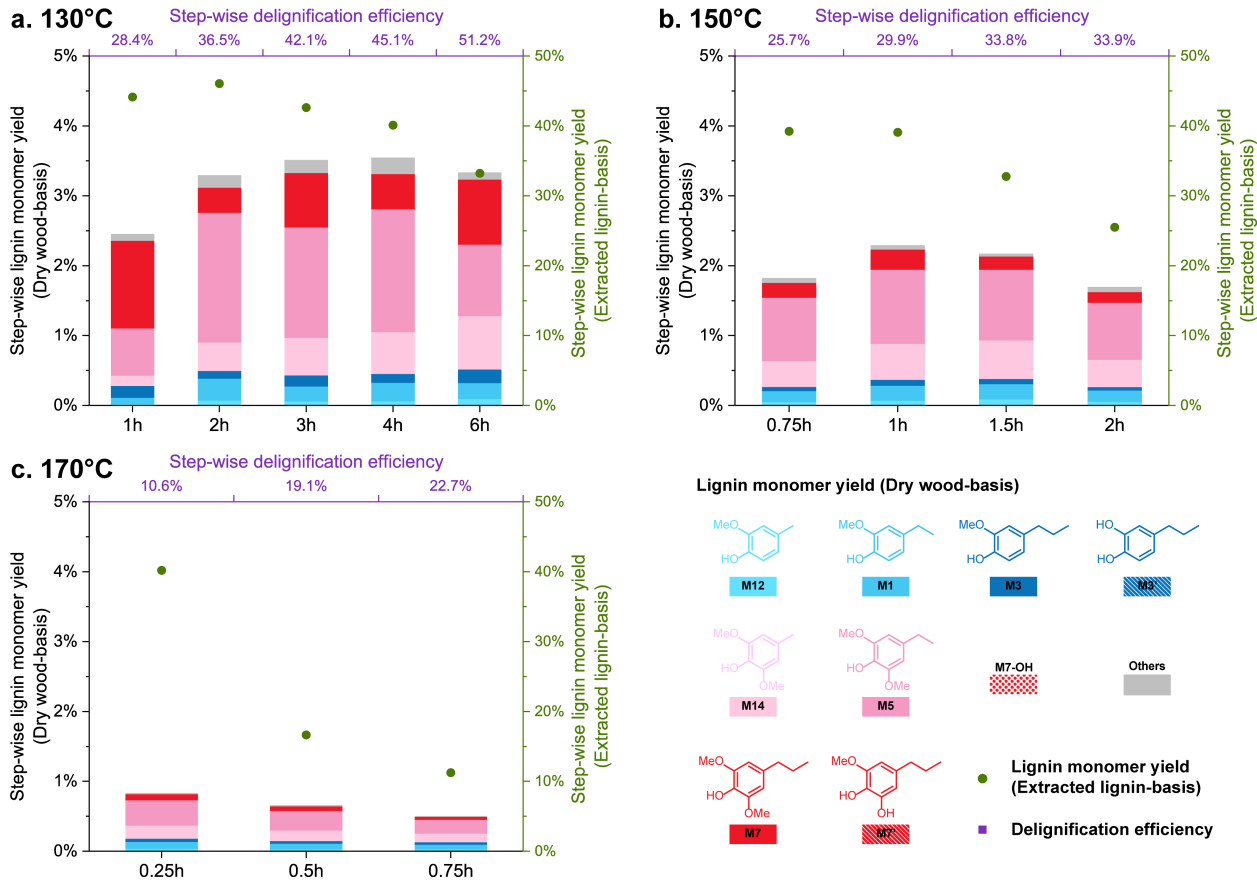


**Figure S10.** Lignin monomer yields through hydrogenolysis and delignification efficiency at each condition optimization stage with varying digestion time. (a) The initial 130°C stage, (b) the second 150°C stage after a fractionation stage at 130°C for 2 h, and (c) the third 170°C stage after a fractionation stage at 130°C for 2 h, and a second fractionation stage at 150°C for 1.5 h. The material loading was 3 g of birch in 50 mL of 1 M NaOH aqueous solution with 0.4 M phenylboronic acid.

#### 4.2.5 Liquor pH change

The pH change in the cooking liquor over time could be attributed to two aspects: 1. acetate hydrolysis from the hemicellulose backbone producing acetic acid, and 2. the peeling reaction of hemicellulose to produce organic acids, such as saccharinic acids.<sup>26</sup> Acetate hydrolysis mostly occurs at the low temperature stages (130°C) while the peeling reaction requires a higher temperature range. From the mass balance analysis of the mix-current configuration (Table S8), almost all detected acetic acid was found in the 130°C stage liquor.

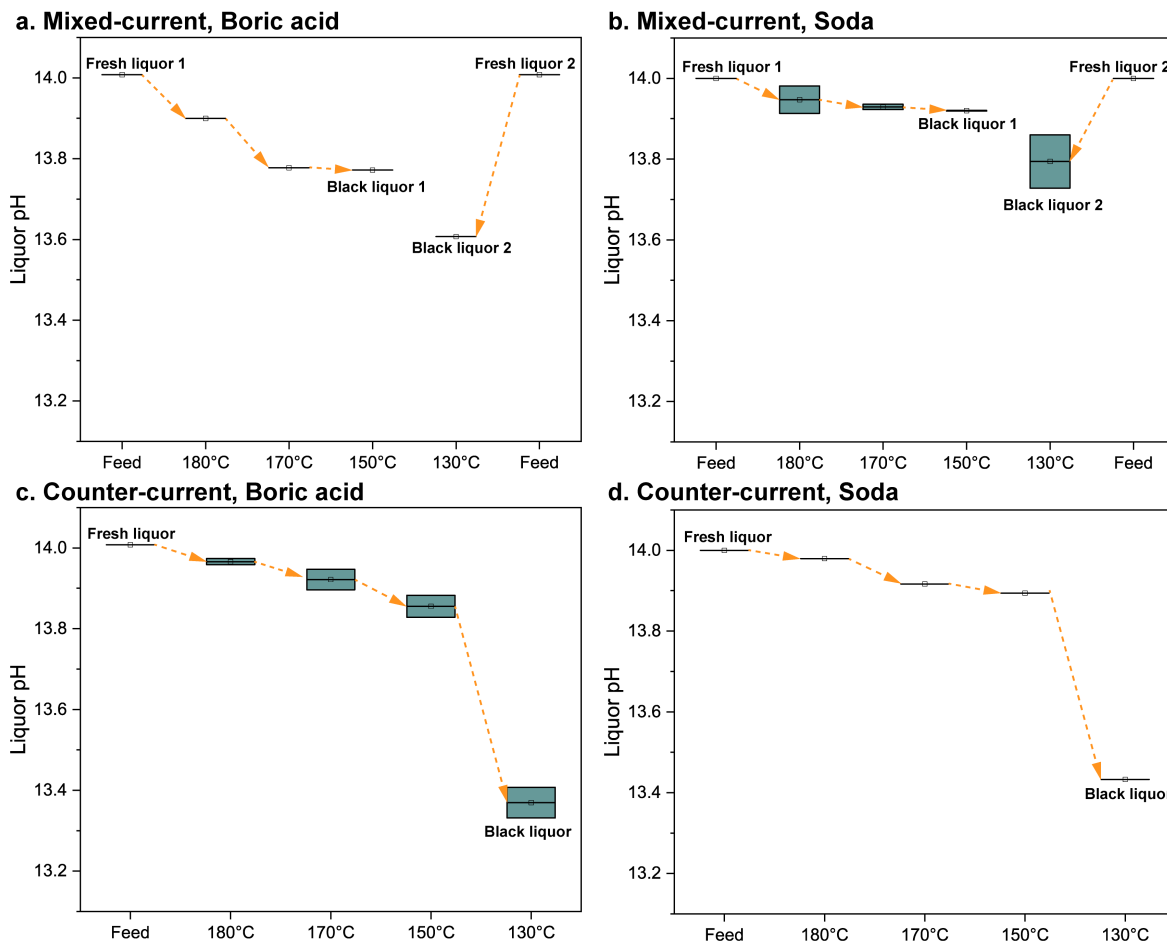


**Figure S11.** The pH of cooking liquor as it progressed through the fractionation process (a) in the mixed-current configuration with boric acid protection, (b) in the mixed-current configuration without protection, (c) in the counter-current configuration with boric acid protection, and (d) in the counter-current configuration without protection. Error margins in b-c panel were calculated from duplicated fractionation experiments.

#### 4.3 Lignin and xylan separation

As briefly explained in the main text, xylan and lignin could be precipitated from the black liquor by either acidification or antisolvent. This work mainly used acidification with HCl for simplicity. CO<sub>2</sub> acidification was also preliminarily tested, as it is the main industrial approach to separating Kraft lignin in the pulping industry.<sup>27</sup> However, the process was very challenging in the lab setup due to the 5-10 bar of CO<sub>2</sub> required throughout the precipitation process. In the study, high pressure could only be achieved during the initial precipitation in a pressurized Parr reactor, but the same pressure could not be maintained during centrifugation and filtration. Due to the high volatility of CO<sub>2</sub> and instability of carbonic acid, any disturbance to the mixture resulted in rapid evaporation of CO<sub>2</sub>, causing the pH to rise in the mixture and lignin to redissolve. The precipitation onset pH was measured to be ca. 8.5, and no further precipitation was seen below pH 5 during HCl acidification. By pressurizing the reactor with 10 bar of CO<sub>2</sub> and stirring the liquor slowly for 30 min, the pH of the mixture reached 5.6 upon depressurizing and opening the reactor, though a lower pH might have been achieved before depressurization. Brown precipitate was observed, while CO<sub>2</sub> continued

to evaporate during liquid transfer. The liquor pH increased to ca. 7 after centrifugation, which was used to separate the precipitate. Vacuum filtration further sped up  $\text{CO}_2$  evaporation, but the pH of the filtrate was between 7.5 and 8 after the operation. As a result of the rising pH, lignin continued to redissolve in the solution. Hydrogenolysis of the  $\text{CO}_2$ -precipitated lignin only produced 47% of lignin monomers compared to HCl-precipitated lignin from the same batch of black liquor (Figure S12). Acidification with  $\text{CO}_2$  would likely be more efficient in a fully enclosed and pressure-tight continuous process, which is common in industrial processing.

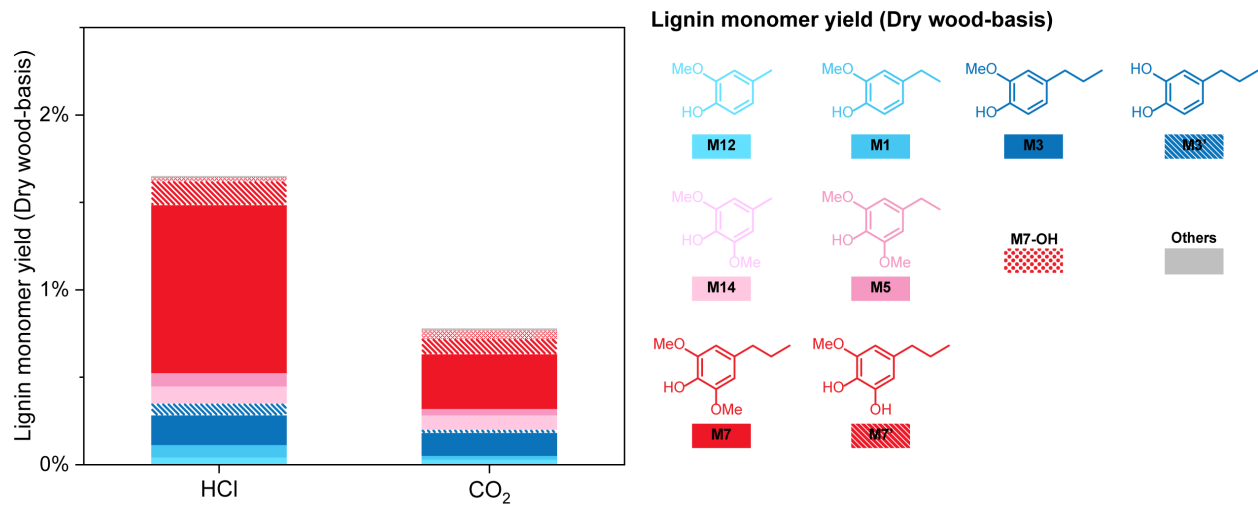


**Figure S12.** Monomer yield comparison of lignin precipitated from the same batch of back liquor with HCl and  $\text{CO}_2$  acidification. Fractionation was performed with birch wood and boric acid protection at  $130^\circ\text{C}$  for 1.5 h after impregnation at  $80^\circ\text{C}$  for 2 h.

Antisolvents provided an additional precipitation method. By screening common solvents, we identified isopropanol as an effective antisolvent to precipitate both lignin and xylan. Ethanol and acetone could precipitate xylan effectively, leaving lignin in the solution, which was also reported in milled wood lignin fractionation.<sup>28</sup>

After precipitation of xylan and lignin with HCl acidification, lignin could be redissolved with organic solvents. Mainly, dioxane was used in this step, since it was also used as the solvent during hydrogenolysis. Less harmful alternatives were also found, such as acetone and ethanol. The  $^1\text{H}$ - $^{13}\text{C}$  HSQC spectra of the lignin and xylan fractions isolated from the mixture using dioxane and acetone are compared in Figure S13. Both solvents achieved good separation of the two components. The spectra of isolated lignin did not show peaks of xylan, and xylan spectra had no noticeable peaks associated with lignin except the peak related to methoxy groups. The isolated xylan also had a consistently over 96% purity, measured by quantitative  $^1\text{H}$  NMR. This selective solubilization method was also effective for lignin-xylan mixture fractionated with both boric acid and phenylboronic acid (Figure S13a-e). A detailed peak identification for xylan and attached methyl galacturonic acid is also shown in Figure S13g. The xylan peak labelling in all other  $^1\text{H}$ - $^{13}\text{C}$  HSQC spectra was simplified due to limited space.

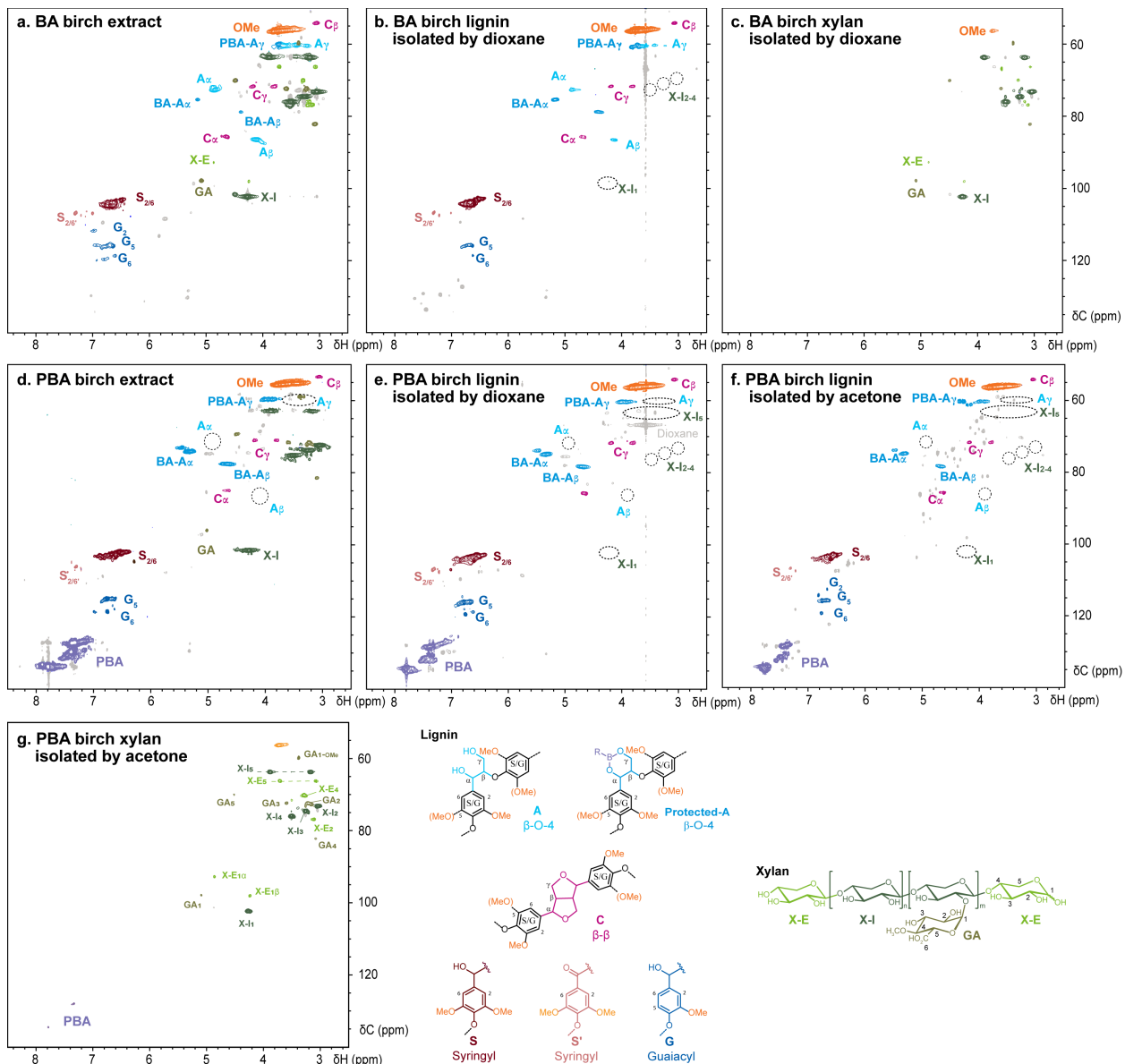


**Figure S13.**  $^1\text{H}$ - $^{13}\text{C}$  HSQC NMR spectra of (a) lignin-xylan mixture obtained from birch with boric acid (BA) at 130°C for 2 h, (b) the lignin and (c) xylan fractions isolated by washing the mixture in (a) with dioxane, (d) lignin-xylan mixture obtained from birch with phenylboronic acid (PBA) at 130°C for 2 h, (e) the lignin isolated by washing the mixture in (d) with dioxane, (f) the lignin and (e) xylan fractions isolated by washing the mixture in (d) with acetone. The detailed peak assignment for the xylan fraction is shown in (g) according to the literature,<sup>23</sup> presented here as a reference for other HSQC spectra. X-E: end unit of xylan, X-I: internal unit of xylan, GA: 4-O-methyl- $\alpha$ -D-glucuronic acid. The dashed circles symbolize the absence of the corresponding peaks.

#### 4.4 Mass balance

Detailed mass balances were developed for the mixed- and counter-current configurations by acid hydrolysis of the solid and liquor fractions (see SI section 3.1). As the fractionation experiments were conducted in duplicates, the compositions in each stream from each trial were measured separately. All measurements were conducted in duplicates to estimate the error margin as the standard deviation, listed in the tables and figures below and in Figure 2 in the main

text). All sugar contents in the liquor were oligomers, as no sugar monomers were detected before liquor hydrolysis. The average values were plotted in Figure 3 in the main text, and tabulated compositions in each stream are summarized in Table S8-9 for biomass components and Table S10-11 for boric acid.

Importantly, boric acid was found to be unassociated with other molecules in the clean liquor, as the BA concentrations were directly measured from the liquor after lignin-xylan precipitation before liquor hydrolysis. This offers an added advantage to BA recycling. No boric acid was detected using HPLC in the cellulose hydrolysate, suggesting that boric acid was not noticeably associated with cellulose. Therefore, the cellulose properties should not be affected by the potential association with boron species.

**Table S8.** Mass balance of biomass components in the mixed-current configuration.

	<b>KL</b>	<b>Glu</b>	<b>Xyl</b>	<b>Gal</b>	<b>Ara</b>	<b>Man</b>	<b>Acetyl</b>
<b>Biomass loading (g)</b>	<b>1.8</b>	<b>3.2</b>	<b>1.8</b>	<b>0.2</b>	<b>0.06</b>	<b>0.03</b>	<b>0.59</b>
<b>Liquor 130(g)</b>		0.04 ± 0.01	0.07 ± 0.01	0.06 ± 0.00	0.01 ± 0.00	0.01 ± 0.00	0.36 ± 0.00
<b>Liquor 150-180(g)</b>		0.02 ± 0.00	0.07 ± 0.01	0.01 ± 0.00	0.00 ± 0.00	0.00 ± 0.00	0.01 ± 0.00
<b>Xylan 130 (g)</b>			0.51 ± 0.01 96% pure				
<b>Xylan 150-180 (g)</b>			0.59 ± 0.18 98% pure				
<b>Pulp (g)</b>	0.02 ± 0.01	3.09 ± 0.05	0.43 ± 0.01	0.05 ± 0.01	0.01 ± 0.00	0.01 ± 0.00	0.00 ± 0.00
<b>% Collected</b>	1.1%	96%	24%	24%	21%	22%	0.00%
<b>Total collected (g)</b>	*	<b>3.2 ± 0.1</b>	<b>1.7 ± 0.2</b>	<b>0.11 ± 0.01</b>	<b>0.02 ± 0.00</b>	<b>0.01 ± 0.00</b>	<b>0.36 ± 0.00</b>
<b>% Collected</b>	*	<b>98%</b>	<b>94%</b>	<b>57%</b>	<b>41%</b>	<b>22%</b>	<b>62%</b>

“KL” refers to Klason lignin; “Glu” refers to glucan; “Xyl” refers to xylan; “Gal” refers to galactan; “Ara” refers to arabinan; and “Man” refers to mannan.

\*The total collected Klason lignin was not listed as the concentration of the lignin solution was not quantified.

**Table S9.** Mass balance of biomass components in the counter-current configuration.

	<b>KL</b>	<b>Glu</b>	<b>Xyl</b>	<b>Gal</b>	<b>Ara</b>	<b>Man</b>	<b>Acetyl</b>
<b>Biomass loading (g)</b>	<b>1.8</b>	<b>3.2</b>	<b>1.8</b>	<b>0.2</b>	<b>0.06</b>	<b>0.03</b>	<b>0.59</b>
Liquor (g)		0.08 ± 0.01	0.12 ± 0.01	0.09 ± 0.01	0.01 ± 0.00	0.00 ± 0.00	0.33 ± 0.01
Xylan (g)			0.88 ± 0.11 98% pure				
Pulp (g)	0.04 ± 0.01	3.1 ± 0.05	0.45 ± 0.01	0.04 ± 0.00	0.01 ± 0.00	0.01 ± 0.00	0.00 ± 0.00
% Collected	2.4%	95%	25%	18%	20%	19%	0.03%
<b>Total collected (g)</b>	*	<b>3.1 ± 0.1</b>	<b>1.5 ± 0.12</b>	<b>0.13 ± 0.01</b>	<b>0.02 ± 0.00</b>	<b>0.01 ± 0.00</b>	<b>0.33 ± 0.00</b>
<b>% Collected</b>	*	<b>98%</b>	<b>81%</b>	<b>65%</b>	<b>44%</b>	<b>19%</b>	<b>57%</b>

“KL” refers to Klason lignin; “Glu” refers to glucan; “Xyl” refers to xylan; “Gal” refers to galactan; “Ara” refers to arabinan; and “Man” refers to mannan.

\*The total collected Klason lignin was not listed as the concentration of the lignin solution was not quantified.

**Table S10.** Mass balance of boric acid in the mixed-current configuration.

	<b>130°C step</b>	<b>150-180°C steps</b>
<b>BA loading (g)</b>	<b>1.22</b>	<b>2.00</b>
Liquor (g)	1.18 ± 0.01	1.96 ± 0.00
Lignin (g)	0.03 ± 0.00	0.04 ± 0.00
Pulp (g)	0.00 ± 0.00	0.00 ± 0.00
<b>Total collected (g)</b>	<b>1.22 ± 0.01</b>	<b>2.00 ± 0.00</b>
<b>% Collected</b>	<b>99.7%</b>	<b>99.9%</b>

**Table S11.** Mass balance of boric acid in the counter-current configuration.

	<b>Full sequence</b>
<b>BA loading (g)</b>	<b>1.27</b>
Liquor (g)	1.23 ± 0.03
Lignin (g)	0.03 ± 0.00
Pulp (g)	0.00 ± 0.00
<b>Total collected (g)</b>	<b>1.26 ± 0.03</b>
<b>% Collected</b>	<b>99.7%</b>

#### 4.5 Boric acid deprotection

Interestingly, over 97% of boric acid remained unreacted in the clean liquor after precipitating lignin and xylan with HCl acidification, and only 2-3% was found in lignin. Considering that total BA loading was approximately 3.5 mol. equivalent to the lignin  $\beta$ -O-4 content in the counter-current case and 8.6 mol. equivalent in the mixed-current case, only 10-20% of  $\beta$ -O-4 was protected with boric acid after isolation, assuming all boric acid in the lignin fraction was associated with the linkages. This corroborates well with lignin HSQC spectra, where lignin extracted with boric acid showed large unmodified  $\beta$ -O-4 cross peaks, whereas no unprotected  $\beta$ -O-4 linkages were detected in lignin extracted with phenylboronic acid (Figure 1c-d). However, this appears to contradict the high monomer yields after hydrogenolysis of both types of lignin (i.e., 39% with boric acid and 45% with phenylboronic acid on an extracted lignin basis, see Figure 2a). If boric acid protection was indeed so ineffective during fractionation, the lignin monomer yield should have approached that of the soda control without the protecting agent. We attribute this to the different propensities to acid hydrolysis of the boric and phenylboronic esters during precipitation instead of the protection effectiveness during alkaline fractionation. Boric esters were found to strongly favour hydrolysis in acidic conditions with a rate constant 10-time higher than that of phenylboronic esters at room temperature.<sup>25</sup> This means that boric acid protection was likely removed from lignin during acid precipitation.

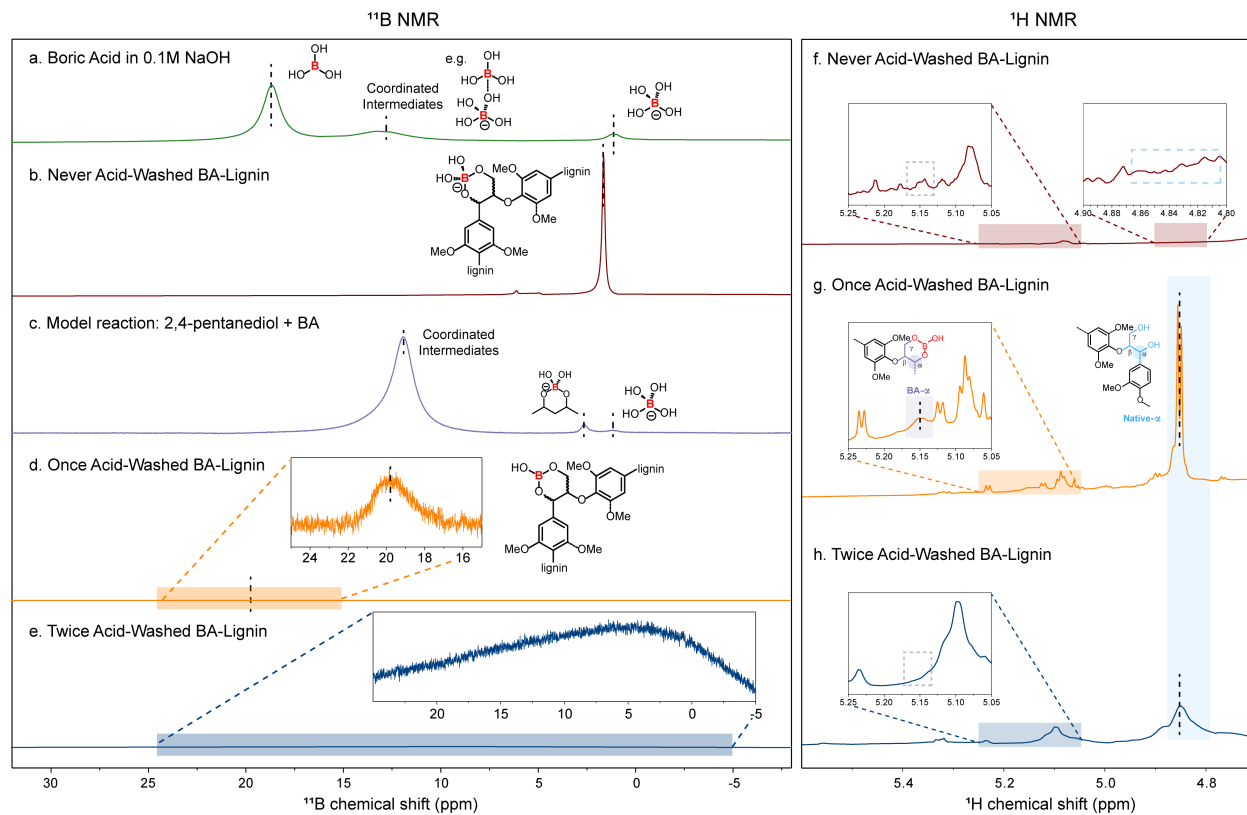


**Figure S14.**  $^{11}\text{B}$  NMR spectra of (a) boric acid in 0.1M NaOD, (b) never acidified lignin, (c) 2,4-pentanediol and boric acid model reaction in 0.1M NaOD at 60°C for 1 h, (d) once acid-washed lignin and (e) twice acid-washed lignin.  $^{11}\text{B}$  peaks assigned according to the literature report.<sup>29,30</sup>  $^1\text{H}$  NMR spectra of (f) never acidified lignin, (g) once acid-washed lignin and (h) twice acid-washed lignin.  $^1\text{H}$  peaks assigned according to literature reports.<sup>5,23,29</sup> Each stack of spectra, except the insets, was plotted with the same scaling factor. Lignin samples of similar masses were loaded for the analysis.

To directly support this hypothesis, we compared the  $^{11}\text{B}$  NMR of boric acid in NaOH solution, never acidified BA-lignin, and once or twice acid-precipitated BA-lignin (Figure S14).  $^{11}\text{B}$  peak assignment was based on literature reports.<sup>29,30</sup> The significantly different  $^{11}\text{B}$  chemical shifts before and after lignin acidification resulted from the reversible hydroxide ion coordination with boron at different pH values.<sup>29</sup> The never acidified lignin was prepared with direct antisolvent precipitation using acetone (Figure S14b). This lignin-xylan precipitate was then dissolved using  $\text{D}_2\text{O}$  and reprecipitated in acetone-d6 twice to remove the effect of  $^1\text{H}$  on NMR spectra. Without neutralization, lignin precipitated as the sodium lignin borate ester salt with one major NMR peak at 1.7 ppm corresponding to cyclic borate ester,<sup>29</sup> which is also in the same range as the boric ester of 2,4-pentenediol as a model compound reaction (Figure S14c). Although the exact chemical shift for cyclic borate ester of lignin is not readily available, Van Duin conducted a systematic study of the  $^{11}\text{B}$  chemical shifts of various cyclic boric and borate esters and reported values in the same range, slightly higher than the chemical shift of sodium borate.<sup>29</sup> The BA-lignin precipitated with HCl acidification to pH 3 showed a small peak at 19.9 ppm (Figure S14d), corresponding to the cyclic lignin-boric ester (with a tri-coordinated boron). After redissolving the acid precipitate of lignin with NaOH solution (pH 13) and reprecipitating with HCl to pH, no boron signals could be detected in the lignin sample by  $^{11}\text{B}$  NMR (Figure S14e), suggesting a near complete hydrolysis of boric ester on lignin. The measurements were recorded using the same sequence in the same instrument consecutively, which should have a comparable signal-to-noise ratio.

The BA-protected and unprotected  $\beta-\text{O}-4$  linkages in the three types of lignin samples were further compared through the characteristic peak of the hydrogen on the benzylic carbon in  $^1\text{H}$  NMR (Figure S14f-h). No unprotected  $\beta-\text{O}-4$  linkages were detected in antisolvent precipitated lignin (Figure S14f). As a result of the  $\text{OH}^-$  coordination to boron involved in the never acidified lignin, the chemical shift of the BA-protected  $\beta-\text{O}-4$  significantly differed from the lignin without  $\text{OH}^-$  coordination, overlapping with sugar peaks. In the once-acidified lignin sample, a large peak corresponding to the unprotected  $\beta-\text{O}-4$  linkages appeared around 4.85 ppm with a small peak at 5.15 ppm for the BA-protected  $\beta-\text{O}-4$  linkages (Figure S14g). No BA-protected  $\beta-\text{O}-4$  peaks were detected in twice-acidified lignin, leaving only one large peak for the unprotected  $\beta-\text{O}-4$  linkages (Figure S14h). The  $\beta-\text{O}-4$  content in these lignin samples was thereby quantified using quantitative NMR (Table S12). The BA-protected  $\beta-\text{O}-4$  linkages in the never acidified lignin were quantified using quantitative  $^{11}\text{B}$  NMR following the literature method,<sup>9</sup> while all others were measured with  $^1\text{H}$  NMR. The total  $\beta-\text{O}-4$  content remained around 1.5 mmol/g over the acidification sequence. Remarkably, a sharp drop of 86% in the BA-protected  $\beta-\text{O}-4$  content can be seen between the never-acidified and once-acidified lignin samples, aligned with the qualitative comparison in Figure 1 in the main text and Figure S14. The lignin hydroxyl content was quantified with  $^{31}\text{P}$  NMR. Notedly, the aliphatic OH content was measured to be about ~twice the  $\beta-\text{O}-4$  content in both samples since each  $\beta-\text{O}-4$  linkage has two hydroxyl groups, further confirming the quantification results.

This simple deprotection method would not only considerably facilitate protecting agent recycling but also provide a straightforward method to recover the native hydroxyl groups in lignin. The remaining boric acid in lignin persisted through lignin hydrogenolysis, largely owing to its simple and inorganic nature, making it resistant to various reactive environments (SI, Section 4.5).<sup>31</sup> While removing the protection group from lignin in other protection-chemistry

assisted processes required a much more complex setup and precise control of the reaction conditions,<sup>32</sup> to date, none of them achieved full protecting agent recovery.<sup>17,33</sup>

**Table S12.**  $\beta$ —O—4 content in lignin samples before and after acid wash.

		$\beta$ —O—4 content, mmol/g lignin			Hydroxyl content mmol/g lignin <sup>[d]</sup>			
		BA- $\beta$ —O—4	Unprotected $\beta$ —O—4	Total	Aliphatic	Aromatic	Carboxylic	Total
<b>BAF lignin</b> <b>130°C</b>	Never acidified	1.64 <sup>[a]</sup>	0 <sup>[b]</sup>	1.64			-	
	Once acidified	0.23 <sup>[b]</sup>	1.29 <sup>[b]</sup>	1.52			-	
	Twice acidified	0 <sup>[b]</sup>	1.46 <sup>[b]</sup>	1.46	3.70	1.65	0.71	6.06
<b>BAF lignin 150-180°C</b>	Twice acidified	0 <sup>[b]</sup>	1.01 <sup>[b]</sup>	1.01	2.07	2.37	0.16	4.60
<b>Native lignin <sup>[c]</sup></b>		0	2.53	2.53			-	

<sup>[a]</sup> Measured by quantitative <sup>11</sup>B NMR with 2,4,6-triphenylboroxin as the internal standard.

<sup>[b]</sup> Measured by quantitative <sup>1</sup>H NMR with 1,2,4,5-tetrachloro-3-nitrobenzene as the internal standard.

<sup>[c]</sup> Measured by quantitative <sup>1</sup>H-<sup>13</sup>C HSQC<sub>0</sub> with polystyrene of the internal standard, retrieved from Bourmaud et al.<sup>34</sup>

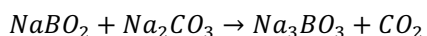
<sup>[d]</sup> Measured by quantitative <sup>31</sup>P NMR as per the protocol of Meng et al.<sup>10</sup> (detailed in Section 3.3)

#### 4.6 Boric acid chemistry

The inorganic nature of boric acid offers a significant advantage over organoboronic acids and other organic protecting agents in lignin-first fractionation. Due to its simple structure, boric acid is not expected to significantly degrade in a wide range of reaction conditions, such as alkaline fractionation, hydrogenolysis and acidic hydrolysis. The near-complete recovery of boric acid also confirmed this hypothesis (Tables S10-11, Figure 3 in the main text).

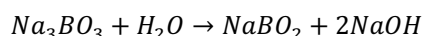
Concerning the integration of BAF into a real pulp mill, though not experimentally investigated, scientific and industrial reports on autocausticizing provided some indications of how boric acid would behave.<sup>31,35</sup> Autocausticizing was proposed to enhance NaOH recovery by adding sodium borate before the black liquor boiler, where organics from biomass are combusted and NaOH reacts with the released CO<sub>2</sub> to form Na<sub>2</sub>CO<sub>3</sub>. By adding sodium borate, this additional chemical can react with Na<sub>2</sub>CO<sub>3</sub> to directly form trisodium borate (Na<sub>3</sub>BO<sub>3</sub>) and release CO<sub>2</sub> (R1 below). After the boiler, the borated smelt is dissolved in water to regenerate NaOH and sodium borate (R2), regenerating NaOH without the need for the calcium cycle that is conventionally required in a chemical pulping plant. The exact speciation of sodium borate in these reactions depended on the ratio between NaOH and sodium borate. If BAF is integrated in a full pulping process, although not experimentally evaluated in this work, we expect that the added boric acid in the NaOH solution would form sodium borate, similar to the direct addition of sodium borate salt in the autocausticizing process. Therefore, the interaction of boric acid and the resulting borate salt is expected to follow a similar path to autocausticizing, which could also enhance liquor recovery.

In the boiler:



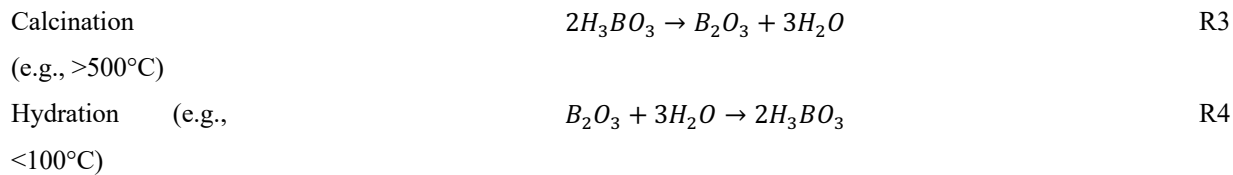
R1

In the dissolving tank:



R2

In addition, unlike phenylboronic acid, boric acid is stable at high temperatures. The most significant reaction that can occur during a calcination cycle is reversible dehydration at elevated temperatures (e.g.  $> 500^{\circ}\text{C}$ , R3), which can be easily hydrated back to boric acid at a low temperature (R4).<sup>36</sup>



In contrast, organoboronic acids are prone to base-catalyzed hydration during fractionation. We conducted control experiments with only phenylboronic acid (PBA) in NaOH solution and heated the mixture at the reaction conditions in a counter-current configuration from  $170^{\circ}\text{C}$  to  $130^{\circ}\text{C}$  (Figure S15). Significant losses of phenylboronic acid were observed due to its hydrolysis to benzene and boric acid (quantified with  $^1\text{H}$  NMR with internal standard), which was also reported previously.<sup>37</sup> Degradation was particularly important at  $170^{\circ}\text{C}$ , consuming 50% of the initial PBA loading after only 15 min, which likely makes PBA unsuitable for fractionation at high temperatures.

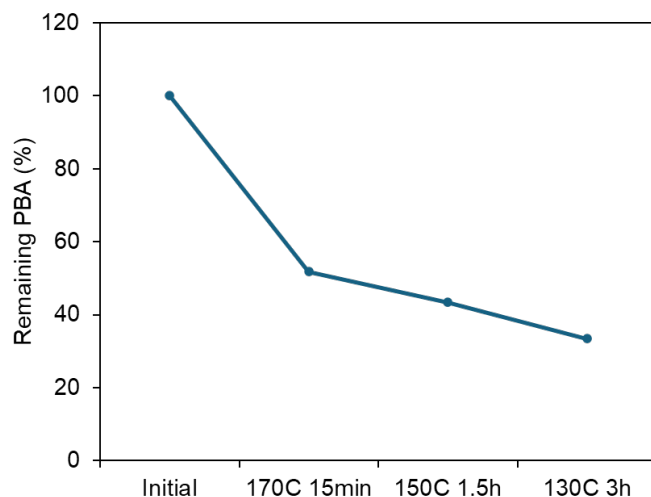


**Figure S15.** The remaining phenylboronic acid (PBA) after each stage in the counter-current BAF condition without biomass loading from  $170^{\circ}\text{C}$  to  $130^{\circ}\text{C}$ .

The degradation of PBA at high temperatures may also explain the difference in monomer yield of lignin extracted with PBA and boric acid using cross-current BAF (Figure S16). Hardwood lignin, including birch and beech, showed a higher monomer yield after hydrogenolysis if the lignin was extracted using PBA, whereas the PBA-protected pine lignin had a lower hydrogenolysis monomer yield than the boric acid-protected alternative. To explain this, we measured the delignification extent at different fractionation temperatures for different wood species. Most hardwood lignin was extracted in the temperature range of  $130\text{--}150^{\circ}\text{C}$ , while pine lignin was predominantly extracted in a much higher temperature range between  $170^{\circ}\text{C}$  and  $180^{\circ}\text{C}$  (Table S5). Therefore, the overall protection effectiveness of PBA on softwood lignin was compromised by the severe degradation of the protecting group in the temperature range where most pine lignin was extracted.

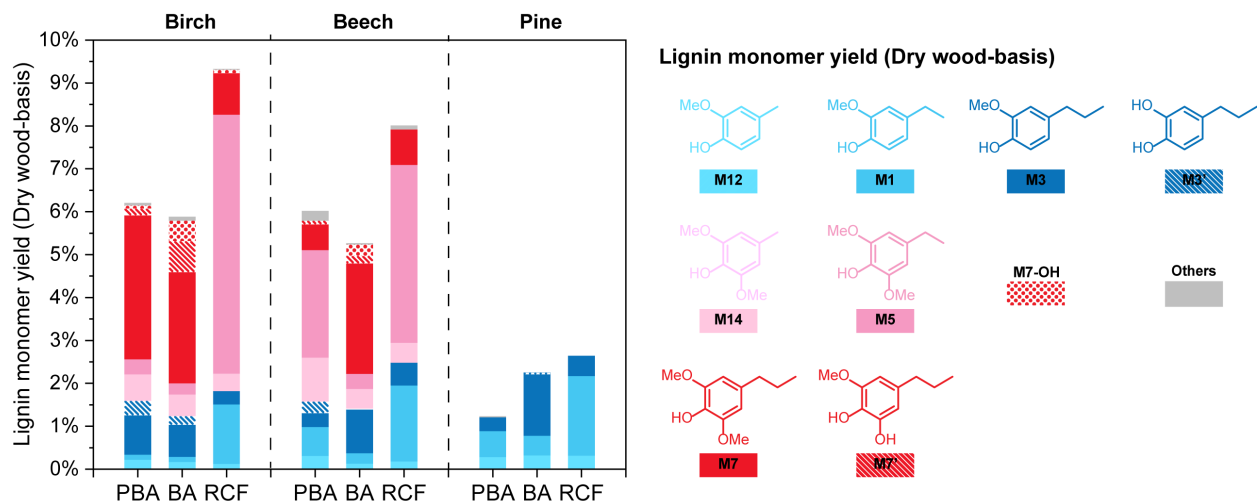


**Figure S16.** The hydrogenolysis of lignin extracted from different wood species using the cross-current BAF with phenylboronic acid (PBA) and boric acid (BA) protection. The results are compared with the RCF lignin monomer yield of the respective wood species.

#### 4.7 Fractionation in the 1 L reactor

Compared to the BAF trials conducted in the 100 mL reactor, the 1 L batches experienced significantly higher heat transfer resistance due to the larger volume-to-surface ratio in the 1 L reactor. Heating and cooling took 30 min to 1 h, compared to below 20 min in the case of the small reactor without stirring. To improve heat transfer, gentle stirring (ca. 60 rpm) was used, trying not to affect the fibre quality by exerting excessive shear during fractionation, which may have caused minor fibrillation and fibre breakage in the prepared pulp (Figure 4 in the main text).

Another effect of the slower heating and cooling in the 1 L reactor was found in the lignin monomer yield (Figure S17). With a similar delignification efficiency, birch-wood lignin extracted in the small batch had a higher overall monomer yield after hydrogenolysis than in the large 1 L batch, which may be attributed to lignin degradation during the extended heating and cooling. However, spruce fractionation in the large reactor achieved higher lignin removal and a slightly higher monomer yield. In this case, we propose that the longer heating and cooling time in the large reactor may act like an impregnation stage, which ultimately improved the overall lignin extraction efficiency, which likely led to a slightly higher total monomer yield of all 4 lignin fractions. In fact, the lignin monomer yields normalized by the delignification efficiency remained comparable between small and large batches for spruce (2.8% vs. 2.7%, respectively). This highlights the need for targeted condition optimization for each case. The lower spruce loading in the 1 L reactor compared to the 100 mL reactor (0.11 vs 0.2 g wood/mL liquor) could also contribute to the improved delignification. The hydrogenolysis monomer yield from lignin extracted at each stage is summarized in Table S13.

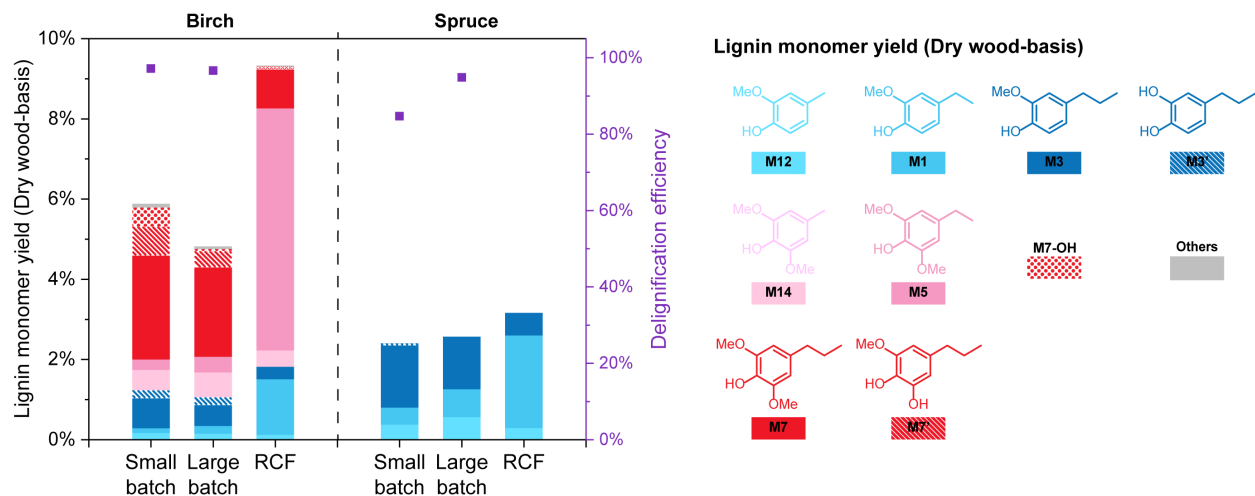


**Figure S17.** Lignin monomer yield comparison between small and large batch experiments using the cross-current BAF with boric acid protection. The results are compared with the RCF lignin monomer yield of the respective wood species.

**Table S13.** Hydrogenolysis monomer yields of lignin extracted from birch and spruce in the 1 L reactor.

Entry	Temp.	Lignin monomer yield % (dry wood-basis)										Delignification efficiency (%)
		stage	M12	M1	M3	M3'	M14	M5	M7	M7'	M7-OH	
<b>Cross-current Birch fractionation with boric acid protection in 1 L fractionation</b>												
1	130°C	0.04	0.07	0.17	0.07	0.10	0.08	0.96	0.14	0.02	0.01	-
2	150°C	0.05	0.06	0.19	0.10	0.19	0.11	0.85	0.15	0.03	0.01	-
3	170°C	0.04	0.04	0.12	0.01	0.20	0.13	0.31	0.05	0.00	0.04	-
4	180°C	0.03	0.02	0.04	0.02	0.13	0.07	0.11	0.07	0.00	0.01	-
	Sum	0.15	0.19	0.52	0.20	0.62	0.39	2.23	0.41	0.05	0.07	96.63
<b>Cross-current Spruce fractionation with boric acid protection in 1 L fractionation</b>												
5	130°C	0.11	0.14	0.46	0.00	0.00	0.00	0.00	0.00	0.00	0.00	-
6	150°C	0.14	0.17	0.24	0.00	0.00	0.00	0.00	0.00	0.00	0.00	-
7	170°C	0.16	0.20	0.36	0.00	0.00	0.00	0.00	0.00	0.00	0.00	-
8	180°C	0.16	0.18	0.25	0.00	0.00	0.00	0.00	0.00	0.00	0.00	-
	Sum	0.57	0.70	1.30	0.00	0.00	0.00	0.00	0.00	0.00	0.00	94.82

#### 4.8 Pulp and handsheet characteristics

**Table S14.** The yield and compositions of pulp produced from large-batch BAF.

Pulp	Yield (g)	Compositions (%)						
		Glucan	Xylan	Galactan	Arabinan	Mannan	Lignin	Sum
Birch unbleached	4.8	78.29	14.87	0.09	0.19	0.07	1.40	94.91
Birch bleached	46.92	78.95	15.53	0.05	0.23	0.12	0.51	95.40
Spruce unbleached	5.49	87.20	4.92	0.10	0.36	4.26	3.71	100.57
Spruce bleached	19.19	86.84	4.66	0.04	0.28	4.19	1.82	97.82

**Table S15.** Characteristics pf BAF pulp compared with industrial Kraft pulp.

Kappa number (-)	Schopper- Riegler number (°SR)	Length (mm)			Mean width (μm)	Aspect ratio
						(-)
Birch Kraft	-	19.5 ± 0.1		1.07 ± 0.01	21.0 ± 0.01	50.8 ± 0.5
Birch BAF bleached	3.5 ± 0.0	16.6 ± 0.4		1.15 ± 0.01	17.4 ± 0.01	66.1 ± 0.6
Birch BAF unbleached	6.6 ± 0.1	-		-	-	-
Softwood Kraft	-	14.5 ± 0.7		2.58 ± 0.02	28.0 ± 0.2	92.1 ± 1.7
Spruce BAF bleached	6.8 ± 0.4	18.8 ± 0.7		1.87 ± 0.00	26.5 ± 0.3	70.4 ± 0.9
Spruce BAF unbleached	21.6 ± 0.3	-		-	-	-

**Table S16.** Characteristics of handsheets made of BAF pulp and industrial Kraft pulp.

	Brightness (%)	Thickness	Grammage	Breaking length	Tensile
		(μm)	(g/m <sup>2</sup> )	(km)	index (Nm/g)
Birch Kraft	83.5 ± 0.1	105.7 ± 1.5	61.9 ± 0.8	2.84 ± 0.04	27.88 ± 0.43
Birch BAF bleached	79.0 ± 0.2	155.6 ± 1.0	60.3 ± 0.2	2.03 ± 0.06	19.91 ± 0.56
Softwood Kraft	83.0 ± 0.2	118.6 ± 2.5	59.9 ± 0.6	2.47 ± 0.05	24.22 ± 0.48
Spruce BAF bleached	76.5 ± 0.2	122.3 ± 1.8	60.5 ± 0.4	3.51 ± 0.14	34.42 ± 1.33

The kappa number is traditionally used in the pulp and paper industry to indicate the residual lignin content in pulp and to estimate how much bleaching is required to obtain the desired brightness in the finished product. While there is no universal correlation between the lignin content and the kappa number or a clear threshold to define bleachability, a kappa number below 35 is generally required for softwood Kraft pulp and 25 for hardwood pulp before bleaching.<sup>22</sup> After fractionation and before bleaching, birch and spruce BAF pulp had kappa numbers of 6.6 and 21.6, respectively, well within the bleachable grade.

The fibre length and width of both BAF pulp samples were in the same range as Kraft references obtained from industry (Table S15, also see microscopy imaging in Figure S18). Minor differences might stem from the different

wood sources used in the pulp mill versus those used in the lab. Birch fibres were thinner and shorter than spruce fibres, which was a known characteristic of industrial hardwood pulp compared to the softwood counterpart.<sup>38</sup>

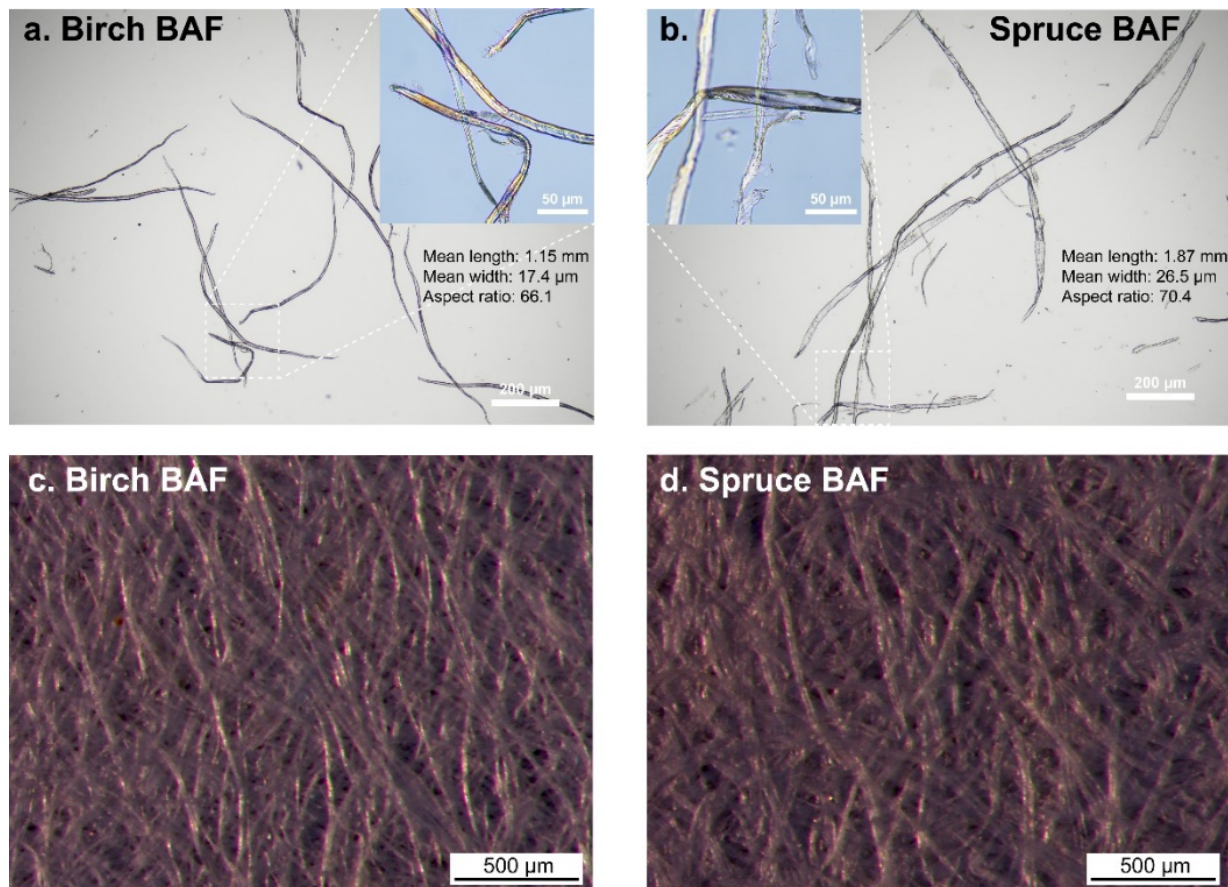


**Figure S18.** Optical microscopic imaging of bleached (a) birch and (b) spruce BAF pulp fibres in suspension, and the handsheet surface made of (c) birch BAF pulp and (d) spruce BAF pulp. Pulp dimensional analysis from FQA is included in panels (a)-(b).

There is a well-established positive correlation between the Schopper-Riegler number ( $^{\circ}$ SR) and pulp's mechanical strength.<sup>38</sup> Spruce BAF pulp, with a higher SR number than softwood Kraft pulp, exhibited a higher tensile index as well, while birch BAF pulp had a slightly lower mechanical strength, which coincided with a lower  $^{\circ}$ SR (Tables S15-16). The handsheet tensile index and pulp's SR number measured in this work are mapped against the typical industrial range for bleached hardwood and softwood Kraft pulp in Figure 4c in the main text. The typical industrial ranges were adapted from a review by de Assis *et al.*,<sup>39</sup> where they mapped the correlation between Canadian standard freeness and breaking length of many industrial pulp samples. To simplify the plot, we summarized the curve clusters with an area, superimposed with the original data retrieved from the literature in Figure S19.

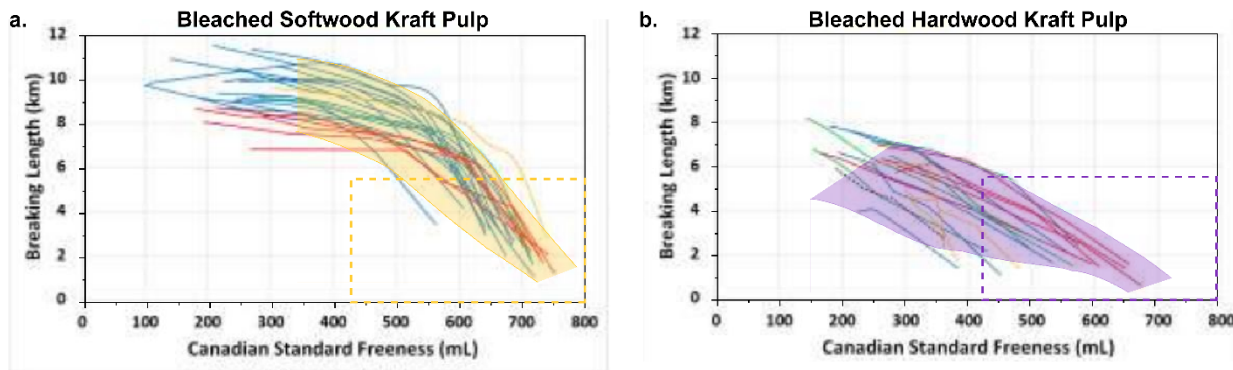


**Figure S19.** The correlation of handsheet breaking length and Canadian standard freeness of the pulp for bleached (a) softwood and (b) hardwood Kraft pulp, summarized by de Assis *et al.*<sup>39</sup> The original figure is reproduced and adapted by adding the coloured regions used to summarize the property ranges for each pulp type. The breaking length was converted to tensile indices using equation S3 and the Canadian Standard Freeness was converted to Schopper-Riegler number plotted in Figure 4c in the main text. The dashed boxes represent the plotted range in Figure 4c.

To facilitate the comparison with the pulp and handsheet characterization in this work, these mapped regions were converted to tensile indices and Schopper-Riegler number. According to equations S1 and S2, the breaking length can be converted to the tensile index using equation S3. The conversion between Canadian standard freeness (CSF) and Schopper-Riegler number ( $^{\circ}$ SR) was conducted by interpolation of the data in Table S17, which was retrieved from the Handbook of Pulp.<sup>40</sup> Note that Schopper-Riegler number and the Canadian standard freeness are two sets of standard measurements with inverted scales, commonly used in Europe and North America, respectively.

In general, pulp freeness is a combined result of the feedstock's intrinsic properties, the pulping process, as well as the post-pulping processing, such as mechanical beating to induce pulp fibrillation.<sup>40</sup> Increasing fibrillation can improve the mechanical strength of the resulting paper.<sup>40</sup> In the absence of post-fractionation beating in this work, the deviation between the Kraft references and the two BAF pulp samples is likely a result of wood sources and the fractionation process itself. The industrial Kraft pulp was acquired from Finland, which was produced using the Nordic wood, whereas the wood chips used in BAF were harvested in Switzerland in Central Europe. The geographical and climatic differences could lead to differences in the intrinsic wood structures and fibre compositions.<sup>22</sup> Therefore, to make a more direct comparison, we wanted to show that all samples were in the expected correlation ranges for commercial paper-grade pulps.

$$\text{Tensile index} = \text{Breaking length} \times \text{gravitational acceleration}$$

S3

**Table S17.** Conversion between Canadian standard freeness (CSF) and Schopper-Riegler number (°SR).

CSF	°SR
800	11.5
775	12.5
750	13.5
725	14.5
700	15.5
675	16.5
650	17.5
625	18.6
600	20.0
575	21.0
550	22.5
525	23.7
500	25.3
475	26.7
450	28.5
425	30.0
400	32.0
375	34.0
350	36.0
325	38.0
300	40.3
275	43.0
250	45.4
225	48.3
200	51.5
175	54.8

The compositions of BAF cellulose obtained from various wood species using the cross current configuration in the 1 L and 100 mL are summarized in Tables S14 and S18, respectively. The compositions of the birch pulp were similar between the two fractionation scales, whereas spruce pulp contained more unextracted Klason lignin and hemicellulosic species, like galactan and arabinan, after the small-scale extraction, likely related to the aforementioned soaking effect and/or the lower solid loading in the large-scale fractionation. On the other hand, beech and pine, though only tested in the small scale, yielded pulp of similar compositions to their respective hand- and softwood analogues, birch and spruce pulp.

**Table S18.** Compositional analysis of 100 mL batch pulp samples using 10 g biomass without bleaching.

	Birch	Beech	Spruce	Pine
<b>Cellulose yield (g)</b>	3.97	3.90	4.05	3.23
Glucan	77.1	74.3	68.0	66.4
Xylan	10.0	10.2	4.5	5.3
Galactan	1.2	1.5	1.9	1.7
Arabinan	0.1	0.1	4.3	2.6
Mannan	0.3	0.7	4.2	2.6
Lignin	1.3	1.1	8.8	13.4
total	90.0	87.8	91.7	92.0

## 5. Comparison with other fractionation technologies

**Table S19.** Fractionation condition comparison between pulping technologies

	Soda <sup>22</sup>	Kraft <sup>22</sup>	BAF
pH range	13-14	13-14	14
Active reagents	NaOH (25-60 g/L)	NaOH (90-110 g/L), Na <sub>2</sub> S (30-45 g/L)	NaOH (40 g/L), boric acid (12 g/L)
Max temperature	155-175°C	155-175°C	170-180°C
Time at max temperature	120-300 min	60-120 min	15-45 min
Total duration	180-360 min	120-270 min	240-320 min
Liquor-to-wood ratio	4:1-8:1	3:1-5:1	10:1 to 5:1*
Delignification	80-90%	>85%	>95%

\* In the mixed-current or counter-current configuration.

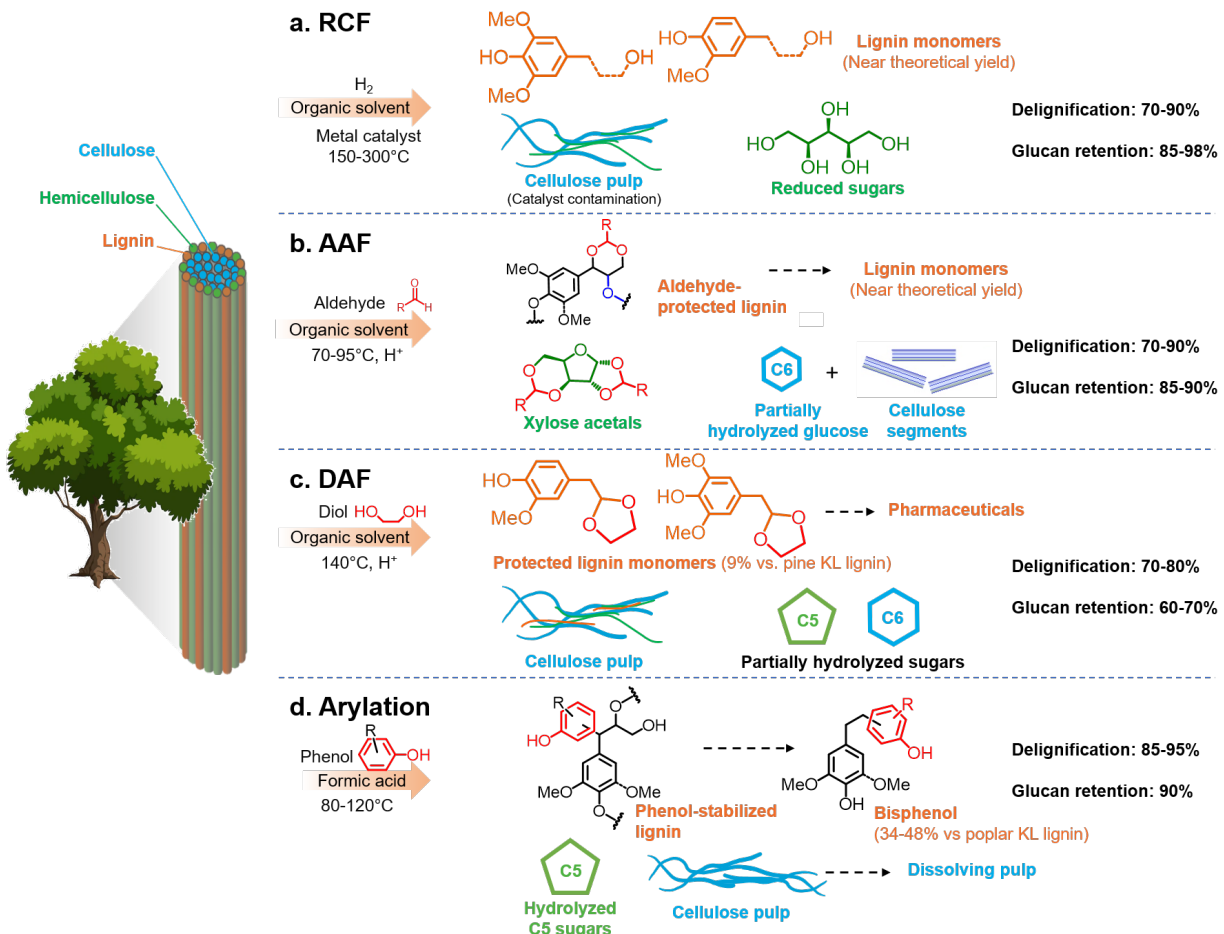


**Figure S20.** Lignin-first biomass fractionation strategies from literature. (a) Reductive catalytic fractionation (RCF),<sup>41</sup> (b) aldehyde-assisted fractionation (AAF),<sup>5,7</sup> (c) diol-assisted fractionation (DAF),<sup>42</sup> and (d) catalytic lignin-arylated fractionation.<sup>43</sup> The fate of lignin and carbohydrates is contrasted between different processes, particularly with respect to the change in lignin structure, the extraction efficiency, and the hydrolysis extent of polysaccharides. Quantitative data retrieved from the respective references.

## 6. Lignin-based adhesive

### Preparation of lignin

BAF and soda lignin was extracted and purified from birch wood using the cross-current configuration detailed in Section 2.2.1.2. BAF lignin was deprotected by acidification prior to adhesive formulation. The three fractions extracted from 150-180°C were combined for the adhesive test.

AAF lignin was produced according the reported procedure using formaldehyde as the protecting agent.<sup>3,44</sup> Briefly, birch wood chips (18 g) were fractionated at 95°C for 3.5 h with formaldehyde (37 wt%, 20.8 mL) as the protecting agent in 100 mL dioxane, acidified with HCl (37 wt%, 8.4 mL). The extracted lignin was precipitated from the concentrated fractionation liquor using diethyl ether as an antisolvent. Kraft lignin (BioPiva 100) was acquired from the UPM group in Finland.

### Preparation of lignin adhesive

FA lignin and Kraft lignin adhesive were prepared by mixing 200 mg lignin with 800 mg Mill-Q water. BAF lignin and Soda lignin adhesive were prepared by mixing 200 mg lignin with 800 mg Mill-Q water and 500 mg acetone to improve dispersity.

### Lap shear adhesion tests

Lap shear adhesion measurements were conducted using beech wood substrates (100 × 25 × 3 mm). Adhesive (150 mg for FA lignin and Kraft lignin adhesive, 200 mg for BAF lignin and Kraft lignin) was cast onto the surface of a single wood substrate to cover an area of 12 × 25 mm (dry weight: 30 g/m<sup>2</sup>). Subsequently, another beech wood substrate was pressed on the adhesive area. The resulting specimen was placed on the plate of a PINETTE PEI hot presser (LAB 150P) and hot pressed at 1.6 MPa and 190 °C for 8 mins.

Lap shear strength was determined by using a Walter+Bai LFM fitted with a 10 kN load cell. Specimens were placed in the instrument using two steel crossbars to hold each substrate. The crossbars were pulled apart at a rate of 1 mm min<sup>-1</sup>. The resulting adhesive strength in units of megapascals (MPa) was calculated by dividing the maximum force (N) by the joint overlap area (mm<sup>2</sup>) (equation S4). Reported adhesion data represent the mean of a minimum of five measurements each with a different sample.

$$\text{Lap Shear Strength (MPa)} = \frac{\text{Maximum force (N)}}{\text{Adhesion area (mm}^2\text{)}} \quad \text{S4}$$

## 7. References

1. Technical Association of the Pulp and Paper Industry (TAPPI). *Test Method TAPPI/ANSI T 205: Forming handsheets for physical tests of pulp*. (2024).
2. International Organization for Standardization (ISO). *ISO 5269-1:2005: Pulps — Preparation of laboratory sheets for physical testing*. (2005).
3. Talebi Amiri, M., Dick, G. R., Questell-Santiago, Y. M. & Luterbacher, J. S. Fractionation of lignocellulosic biomass to produce uncondensed aldehyde-stabilized lignin. *Nat. Protoc.* **14**, 921–954 (2019).
4. Sluiter, A. *et al. Determination of Sugars , Byproducts , and Degradation Products in Liquid Fraction Process Samples: Laboratory Analytical Procedure*. (2008).
5. Shuai, L. *et al.* Formaldehyde stabilization facilitates lignin monomer production during biomass depolymerization. *Science (80-. ).* **354**, 329–333 (2016).
6. Lan, W., de Bueren, J. B. & Luterbacher, J. S. Highly Selective Oxidation and Depolymerization of  $\alpha,\gamma$ -Diol-Protected Lignin. *Angew. Chemie Int. Ed.* **58**, 2649–2654 (2019).
7. Lan, W., Amiri, M. T., Hunston, C. M. & Luterbacher, J. S. Protection Group Effects During  $\alpha,\gamma$ -Diol Lignin Stabilization Promote High-Selectivity Monomer Production. *Angew. Chemie Int. Ed.* **57**, 1356–1360 (2018).
8. Dick, G. R., Komarova, A. O. & Luterbacher, J. S. Controlling lignin solubility and hydrogenolysis selectivity by acetal-mediated functionalization. *Green Chem.* **24**, 1285–1293 (2022).
9. Aguilera-Sáez, L. M. *et al.* Pushing the frontiers: Boron-11 NMR as a method for quantitative boron analysis and its application to determine boric acid in commercial biocides. *Analyst* **143**, 4707–4714 (2018).
10. Meng, X. *et al.* Determination of hydroxyl groups in biorefinery resources via quantitative  $^{31}\text{P}$  NMR spectroscopy. *Nat. Protoc.* **14**, 2627–2647 (2019).
11. International Organization for Standardization (ISO). *ISO 302:2015: Pulps — Determination of Kappa number*. (2015).
12. International Organization for Standardization (ISO). *ISO 5267-1:1999/Cor 1:2001: Pulps — Determination of drainability — Part 1: Schopper-Riegler method*. (2001).
13. Technical Association of the Pulp and Paper Industry (TAPPI). *Test Method TAPPI/ANSI T 271: Fiber length of pulp and paper by automated optical analyzer using polarized light*. (2012).
14. International Organization for Standardization (ISO). *ISO 2470-1:2016: Paper, board and pulps — Measurement of diffuse blue reflectance factor Part 1: Indoor daylight conditions (ISO brightness)*. (2016).
15. Technical Association of the Pulp and Paper Industry (TAPPI). *Test Method TAPPI/ANSI T 494: Tensile properties of paper and paperboard (using constant rate of elongation apparatus)*. (2022).

16. Wu, X. *et al.* Advancements and Perspectives toward Lignin Valorization via O -Demethylation. *Angew. Chemie* **136**, (2024).
17. Abu-Omar, M. M. *et al.* Guidelines for performing lignin-first biorefining. *Energy Environ. Sci.* **14**, 262–292 (2021).
18. Li, Z., Sutandar, E., Goihl, T., Zhang, X. & Pan, X. Cleavage of ethers and demethylation of lignin in acidic concentrated lithium bromide (ACLB) solution. *Green Chem.* **22**, 7989–8001 (2020).
19. Bomon, J. *et al.* Efficient demethylation of aromatic methyl ethers with HCl in water. *Green Chem.* **23**, 1995–2009 (2021).
20. Witthayolankowit, K. *et al.* Valorization of Tops and Branches to Textile Fibers and Biofuel: Value Chain Explored Experimentally; Environmental Sustainability Evaluated by Life Cycle Assessment. *ACS Sustain. Chem. Eng.* **12**, 526–533 (2024).
21. Evstigneyev, E. I. & Shevchenko, S. M. Lignin valorization and cleavage of arylether bonds in chemical processing of wood: a mini-review. *Wood Sci. Technol.* **54**, 787–820 (2020).
22. Young, R. A., Kundrot, R. & Tillman, D. A. Pulp and Paper. in *Encyclopedia of Physical Science and Technology* 249–265 (Elsevier, 2003). doi:10.1016/B0-12-227410-5/00619-0.
23. Kim, H. & Ralph, J. A gel-state 2D-NMR method for plant cell wall profiling and analysis: A model study with the amorphous cellulose and xylan from ball-milled cotton linters. *RSC Adv.* **4**, 7549–7560 (2014).
24. Sun, S., Huang, Y., Sun, R. & Tu, M. The strong association of condensed phenolic moieties in isolated lignins with their inhibition of enzymatic hydrolysis. *Green Chem.* **18**, 4276–4286 (2016).
25. Ito, H. *et al.* Kinetic study of the complex formation of boric and boronic acids with mono- and diprotonated ligands. *Inorganica Chim. Acta* **344**, 28–36 (2003).
26. Fearon, O. *et al.* Detailed modeling of the kraft pulping chemistry: carbohydrate reactions. *AIChE J.* **66**, 1–9 (2020).
27. Argyropoulos, D. D. S. *et al.* Kraft Lignin: A Valuable, Sustainable Resource, Opportunities and Challenges. *ChemSusChem* **16**, (2023).
28. Sun, R. C., Mott, L. & Bolton, J. Fractional and structural characterization of ball milled and enzyme lignins from oil palm empty fruit bunch fiber. *Wood Fiber Sci.* **30**, 301–311 (1998).
29. Van Duin, M., Peters, J. A., Kieboom, A. P. G. & Van Bekkum, H. Studies on borate esters 1. *Tetrahedron* **40**, 2901–2911 (1984).
30. Hiraishi, N., Sayed, M., Hill, R., Tagami, J. & Hayashi, F. Interactions of boron released from surface pre-reacted glass ionomer with enamel/dentin and its effect on pH. *Sci. Rep.* **11**, 1–9 (2021).
31. Than, B. H., Mao, X. & Cameron, J. Autocausticizing of smelt with sodium borates. *Pulp Pap. Canada* **100**,

35–40 (1999).

32. Sun, S. *et al.* Integrated Conversion of Lignocellulosic Biomass to Bio-Based Amphiphiles using a Functionalization-Defunctionalization Approach. *Angew. Chemie Int. Ed.* **63**, 1–9 (2024).
33. Liu, Y. *et al.* Tunable and functional deep eutectic solvents for lignocellulose valorization. *Nat. Commun.* **12**, 1–15 (2021).
34. Bourmaud, C. L. *et al.* Quantification of Native Lignin Structural Features with Gel-Phase 2D-HSQC Reveals Lignin Structural Changes During Extraction. *Angew. Chemie Int. Ed.* **63**, (2024).
35. Jma Hoddenbagh, B., WILFING, K., Miller Hardman, K. D. & ThAN, H. Borate autocausticizing: a cost effective technology. *Pulp Pap. Canada* **103**, 16–22 (2002).
36. Künkül, A., Aslan, N. E., Ekmekyapar, A. & Demirkiran, N. Boric Acid Extraction from Calcined Colemanite with Ammonium Carbonate Solutions. *Ind. Eng. Chem. Res.* **51**, 3612–3618 (2012).
37. Liu, Z. *et al.* Phase-transition-induced phosphorescence: A novel icing detection strategy for airplane. *Dye. Pigment.* **223**, 111969 (2024).
38. de Assis, T. *et al.* Comparison of wood and non-wood market pulps for tissue paper application. *BioResources* **14**, 6781–6810 (2019).
39. De Assis, T. *et al.* Understanding the Effect of Machine Technology and Cellulosic Fibers on Tissue Properties – A Review. *BioResources* **13**, 4593–4629 (2018).
40. Sixta, H. Papermaking Properties of Pulps. in *Handbook of Pulp* 1281–1289 (Wiley, 2006). doi:10.1002/9783527619887.ch32.
41. Jang, J. H. *et al.* Feedstock-agnostic reductive catalytic fractionation in alcohol and alcohol–water mixtures. *Green Chem.* **25**, 3660–3670 (2023).
42. De Santi, A., Galkin, M. V., Lahive, C. W., Deuss, P. J. & Barta, K. Lignin-First Fractionation of Softwood Lignocellulose Using a Mild Dimethyl Carbonate and Ethylene Glycol Organosolv Process. *ChemSusChem* **13**, 4468–4477 (2020).
43. Li, N. *et al.* Selective lignin arylation for biomass fractionation and benign bisphenols. *Nature* **630**, 381–386 (2024).
44. Yang, G., Gong, Z., Luo, X., Chen, L. & Shuai, L. Bonding wood with uncondensed lignins as adhesives. *Nature* **621**, 511–515 (2023).